Journal of Materials Chemistry C

ROYAL SOCIETY OF CHEMISTRY

REVIEW

View Article Online
View Journal | View Issue

Cite this: J. Mater. Chem. C, 2023, 11, 9749

Biogenic amine sensors using organic π-conjugated materials as active sensing components and their commercialization potential

Michael J. Grant, Kathryn M. Wolfe, Cayley R. Harding and Gregory C. Welch *

Received 1st February 2023,
Accepted 29th June 2023

DOI: 10.1039/d3tc00383c

rsc.li/materials-c

An overview of biogenic amine sensors using organic π-conjugated active layers is presented. Biogenic amines are released from decomposing food stuffs, in particular meat and fish, and thus the detection of such off gasses can help minimize food waste and prevent the consumption of spoiled foods, reducing illnesses. The creation of real-time food monitoring sensors may replace best before dates and increase the efficiency and effectiveness in how humans treat food. Owing to the importance of this topic, numerous efforts have been put forth to develop biogenic amines sensors. A sub-section includes those based on organic conjugated materials, versatile compounds that can undergo changes to electronic structures upon interaction with the amines. This short review summarizes key findings in the development of colorimetric and fluorescent sensors based upon organic molecules, organic polymers, and covalent organic frameworks. Additionally, some electrochemical sensors are highlighted, of which use organic polymers and carbon nanomaterials in radio-frequency identification, chemiresistive and field-effect transistor-based devices.

10th Anniversary Statement

Over the last 10 years, both the life of the journal and my independent academic career, the *Journal of Materials Chemistry C* has been an important forum to publish my teams research. Our work centers on the development of organic conjugated materials for use in printed electronic devices including photovoltaic cells, light emitting didoes, and field-effect transistors. Some of our first work on exploring structure–property relationships of simple phthalimide based organic materials was published in this journal (*J. Mater. Chem. C*, 2014, **2**, 2612–2621) and started us on a journey that led to the rediscovery of the versatile *N*-annulated perylene diimide building block and the discovery of a cyclic secondary amine functionalized perylene diimide, enabling high voltage indoor photovoltaics cells (*J. Mater. Chem. C*, 2020, **8**, 13430–13438) and air-stable transistors (*J. Mater. Chem. C*, 2021, **9**, 13630–13634), respectively. Core to our work has been a focus on the 'green' synthesis and solution processing of organic conjugated materials with an emphasis on direct heteroarylation and slot-die coating methods, respectively. All this leading up to a special issue on Green Electronics (*J. Mater. Chem. C*, 2022, **10**, 2869–2869) with myself as guest editor. For this feature 10th anniversary issue, we have presented a highlight of a new area my team has entered, that is the development of conjugated organic materials for biogenetic amine sensing. Food security is one of the most important topics in society today and organic materials scientists have an opportunity to make a direct impact.

1. Introduction

Food waste is a major public concern, where it was recently estimated by the United Nations Environment Programme that 931 million tonnes of food was wasted globally in 2019.[1] Additionally, according to the World Health Organization, unintentional consumption of spoiled food resulted in ~600 million people getting sick and ~420 000 deaths in 2010.[2] Currently, expiration dates are used as a means to circumvent liability when consumers fall ill from spoiled food consumption, and do not serve to provide information on the quality of the food product. As a result, expiration dates do not effectively combat premature disposal of food products and even unintentional consumption of spoiled food due to unsafe storage. Efforts are being made to develop sensors that provide more accurate indications of food spoilage compared to best before dates, which would serve to mitigate these issues of food wastage and food-borne illnesses upon implementation in food packaging. A common means to evaluate food quality is to track microbial

Department of Chemistry, University of Calgary, 2500 University Drive N.W., Calgary, Alberta, T2N 1N4, Canada. E-mail: gregory.welch@ucalgary.ca

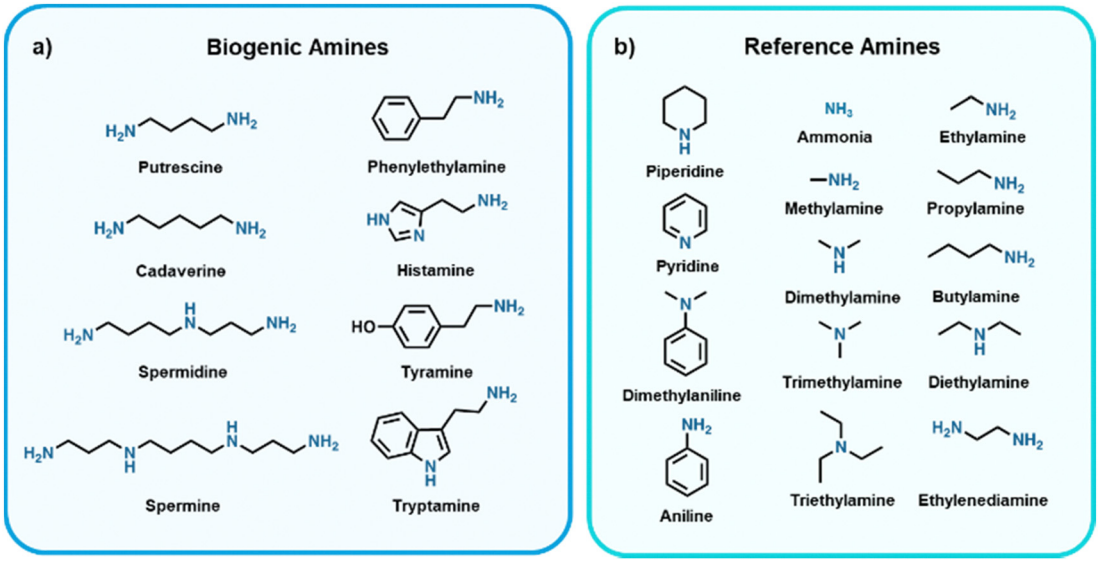

Fig. 1 Structures and names of selected (a) biogenic amines (BAs) and (b) reference amines[34–47] commonly used in laboratory-based settings.

growth,[3] where current sensing methods for estimating/tracking growth for food packaging applications include, but are not limited to, monitoring pH changes,[4–8] changes in temperatures over time,[9–11] O_2 content,[12–15] CO_2 content,[15–18] or biogenic amine (BA) content.[19–22] Produced by bacteria found in food *via* decarboxylation of amino acids, BAs are biomolecules of low molecular weight and are known for their toxic and carcinogenic effects.[23–26] The most commonly found BAs in food are highlighted in Fig. 1a. Since BAs are volatile they can be sensed as gases, which in theory could be integrated into packaging to realize so-called ''smart food packaging'' which serves to improve shelf life, safety, and quality of food products. We refer the reader to some recent reviews for more insight on the progress made to realize smart food packaging as a whole.[27–33] It should be noted that many sensors being developed for BA detection in academic labs tend to use reference amines (Fig. 1b) as the analyte being sensed. Reference amines are used as these have similar structures to BAs and many are found in rotten food, however, do not possess the toxic traits that BAs do and thus are ideal for lab-based testing.

Various modes of sensing gaseous BAs have been reported, some of which are: optical sensors,[48–50] biosensors,[47,51–54] and electrochemical sensors.[37,55–57] First, optical BA sensors exhibit a change in colour and/or fluorescence of the active component in the presence of reference and/or biogenic amines. Secondly, biosensors for BA detection have incorporated enzymes, immunosystems, tissues, organelles, and even whole cells in their active component for the detection of BAs. Lastly, electrochemical BA sensors rely on materials that undergo a measurable change in conductivity upon exposure to reference or biogenic amines. There exists several reviews on the sensors developed over the past two decades to realize BA detection for applications in food packaging,[19–22] however, what is lacking in the literature is a review on the progress made towards realizing commercialization of these sensors. Before considering commercialization, the sensors must meet certain metrics: they should exhibit a response rate to BAs on the order of minutes or less, must be selective to BAs and non-responsive to other analytes, and must have an appropriate limit of detection (LOD), which is the minimum amount of analyte needed to produce a response, where a response must be observed before food is spoiled. The sensitivity, which can be defined as how much the response changes as analyte concentrations increase, is important in the event the sensor aims to provide a dosimeter type response as opposed to an on/off response. Furthermore, sensors must contain non-toxic materials and should be simple to use. Once this has been achieved and a product has been developed, large scale production needs to be viable to reach commercialization, where the materials used must be readily available and/or easily synthesized, low in cost, and use production methods that can be easily scaled with reasonable time, energy, and material input. Organic π-conjugated compounds as the active sensing materials in BA sensors are the sole focus in this review due to their ability to be low-cost, non-toxic, synthesized in large quantities, highly tunable to meet target physical/chemical properties, and ability to form uniform thin films on flexible substrates by printing/coating techniques from ink formulations, as flexible thin films are ideal sensors due to their ease of integration into food packaging. Herein, we highlight the most viable systems for BA sensing for food packaging applications using organic π-conjugated materials and discuss what limitations prevent them from reaching commercialization.

2. Colorimetric sensors

In terms of public accessibility, colorimetric sensors are appealing as they are easily understood being that the sensing response is presented as a change in color. However, this type of response

Table 1 Summary of colorimetric BA sensors

Sensing material(s)	Color change	Sensing mechanism	Source of BAs	LOD	Film substrate/coating method	Ref.
TSCN	Yellow → blue	Acid/Base	Salmon (1 week)	8 ppm (butylamine)[a]	Cellulose/dip-coating	37
MAF	Colourless → red	Ring-opening	Cod (8 hours)	0.5 ppm (DMA)	Nylon membranes/ dip-coating	38
GJM-492	Green → red	Acid/Base	Chicken & pork (1 & 2 days)	1.5 ppm (ammonia)	PET/knife-coating	39
NPTh	Brown → black	Charge transfer	Beef, pork, salmon (3 days)	0.45 ppm (cadaverine)	Glass/spin-coating	31
Rhodamine, Fluorescein	Red → yellow	Nucleophilic attack	Salmon (6 hours)	*Ca.* 0.7 ppm (ammonia)[a]	PET/drop-casting	67
Chalcone functionalized polydiacetylene	Purple → orange[b]	Acid/Base	*Sparus Aurata* (16 hours)	3 ppb (ammonia)	Filter paper/drop-casting	68

[a] No LOD is provided. Value given is the lowest reported to give an observable colour change. [b] At 20 °C. Colour is also dependant on temperature.

needs to provide a significant color change to clearly indicate the point of spoilage. Currently, there exists commercial time-temperature indicators for food packaging applications that act as colorimetric sensors. Some notable time-temperature indicators with significant color changes are: CheckPoint® (green to yellow to red colour change), Fresh-Check® (colorless to blue), On Vu™ (dark blue to colorless), and 3M™ Monitor Mark™ (colorless to blue).[33] It is worth noting that in order to be more inclusive to those that are color blind, a change in shading or pattern is commonly seen in these sensors. As well, phone applications could also be developed to read these types of sensors.

Materials that change color upon applied stimuli are witnessed in many types of materials, however, organic materials offer an advantage as they are highly tunable in terms of the color changes that occur upon applied stimulus. The LOD, which corresponds to the start of the color change response, and the sensitivity can be potentially tuned for organic materials as colorimetric sensors, but is highly dependent on the sensing mechanism itself. One strategy to design sensing materials is to covalently link a chromophore with an analyte receptor, where the receptor when engaged with an analyte induces a color change and provides a means of controlling the performance by choice of chromophore and/or receptor.[58–65] Some other works use acid–base chemistry, as BAs contain basic amine groups, where upon protonation or deprotonation of the chromophore the electronic structure of the material is altered and thus results in a color change.[38,40,66,67] It can then be possible to alter the pK_a or pK_b of the acidic/basic site to adjust the LOD through modifications to the chromophore such as adding or removing functional groups that alter the optoelectronic properties. Another strategy is to induce a chemical change by designing chromophores that are reactive with BAs to change the electronic structure of the compounds, as BAs can be reactive due to their nucleophilic nature.[39,68–70]

In terms of commercialization potential, using colorimetric organic materials as sensing materials are appealing as they possess the ability to be rendered soluble in a range of solvents such that they can be printed on various substrates. This then translates to thin films as color changing sensors that can be mass produced by printing methods, and since these films can be printed on flexible substrates, they are ideal for integration into food packaging. This section focuses on thin film colorimetric sensors made from organic materials as the active sensing component; sensors are summarized in Table 1.

2.1. Organic small molecule-based colorimetric sensors

Weder *et al.* developed a colorimetric sensor based on a thiourea derivative attached to the common naphthalimide chromophore (Fig. 2a).[38] This thiosemicarbazide-naphthalimide (TSCN) compound is yellow in color and facilitates a proton transfer from the thiosemicarbazide group to analytes such as amines (Fig. 2a), causing a change in the electronic configuration of the system. A thiourea-derived receptor was chosen due to its biocompatibility and relatively high acidity,[71] enabling formation of a stable coordination complex.[72] Exposure of TSCN to amines such as butylamine results in a color change from yellow to blue, where the UV-Visible absorption spectrum of TSCN in solution showed a red-shift of over 100 nm of the primary absorption band (*ca.* 416 nm to 574 nm). This color change was found to be reversible upon exposure to acid (trifluoroacetic acid), which re-protonates the chromophore. Solid-state sensors were constructed by dipping cellulose substrates into a solution of the dye (10 mM acetone solution) and then dried under vacuum. Upon exposure to butylamine, the sensors had an instantaneous color change (approx. 2s), which was observable at butylamine vapor concentrations as low as 8 ppm. Generally, upon exposure to other amines with lower vapor pressure, there was a lower intensity of response, therefore, the intensity of the response of these sensors appears to be related to the vapor pressure of the amines tested. Exposure to butylamine (vapor pressure 12.4 kPa) results in a more significant change in color than exposure to triethylamine (7.2 kPa), for example. This inferred that the response time of the sensor was dependent on the concentration of the amines, with the least volatile giving the lowest vapor concentration and slowest response time or lack thereof. These sensors show promise at detecting the more volatile BAs at low concentrations and potential as real-world sensors for fish. Salmon was stored at room temperature for a week allowing for decomposition and exposing the sensor to the fish resulted in a color change from yellow to blue, thus confirming the presence of BAs.

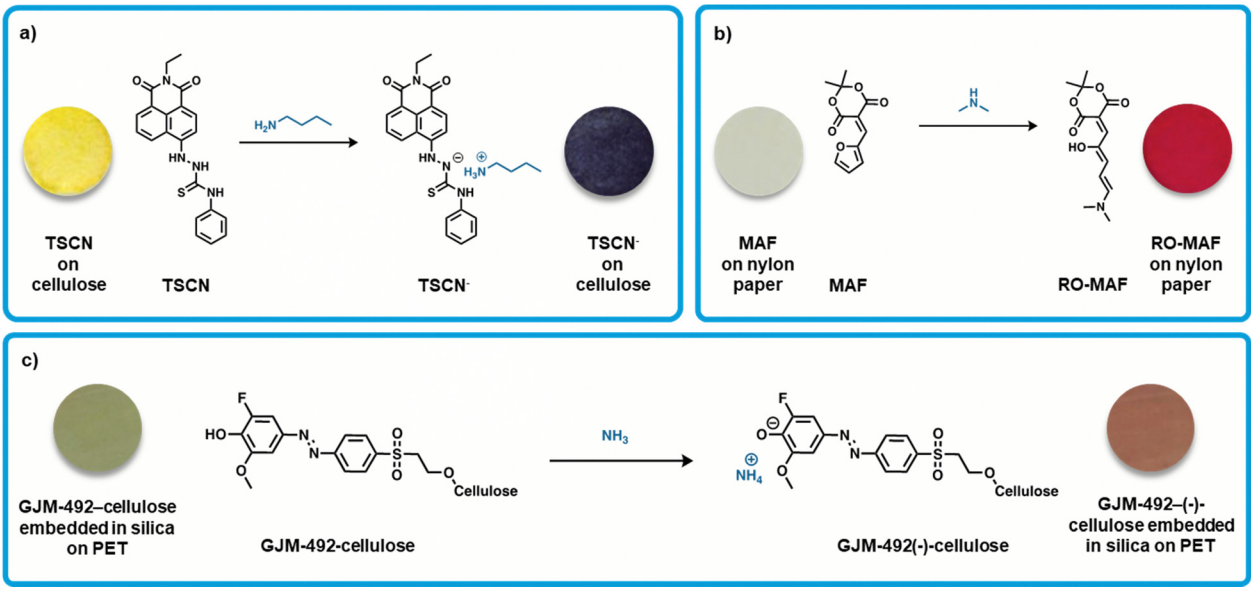

Fig. 2 Organic small-molecule colorimetric amine sensors. (a) Deprotonation of TSCN by butylamine resulting in $[TSCN]^-[butylamine]^+$, inset: modified images of TSCN and $TSCN^-$ on a cellulose substrate with permission from Weder *et al.*[38] (b) Ring opening of the furan moiety on MAF *via* dimethylamine to produce RO-MAF, inset: modified images of MAF and RO-MAF on a nylon paper substrate with permission from Read de Alaniz *et al.*[39] (c) Deprotonation of GJM-492-cellulose with ammonia resulting in GJM-492-(−)-cellulose, inset: modified images of GJM-492-cellulose and GJM-492-(−)-cellulose coated on PET with permission from Mohr *et al.*[40]

Read de Alaniz *et al.* developed a colorimetric sensor that incorporated Meldrum's activated furan (MAF), a furan functionalized with Meldrum's acid, for specific amine gas detection.[39] The active furan-carbon acids are colorless, easily synthesized from low-cost and abundant building blocks, and therefore hold potential for large scale production. Upon exposure to secondary amines, the furan ring-opens forming a thermodynamically stable conjugated donor–acceptor structure, which has an associated strong red color (Fig. 2b). The significant structural change of this mechanism rendered these sensors non-reversible. The sensing devices were fabricated by dipping nylon filter membranes into a solution of the active compound (450 mM THF solution) and then dried. For testing, the sensors were sealed in septa-capped scintillation vials and exposed to gaseous amines. When exposed to dimethylamine vapor (*ca.* 0.3 to 2 ppm), the expected colorless to red color change occurred. Additionally, The International Commission on Illumination (CIE) guidelines were followed to quantify the color difference observed by eye, where ΔE^* values greater than 7 are generally distinguishable by eye.[73–75] Exposure to both dimethylamine and ammonia vapors (*ca.* 0.5 ppm) gave distinguishable color changes ($\Delta E^* > 7$). Of note, exposure of the sensor to secondary amines provides a more striking color change, as compared to non-substituted amines. For example, diethylamine exposure gave a deep red color while ammonia exposure only gave a light pink color, which implies the capability towards specific detection of volatile amines. These sensors were tested briefly with fish samples, and when sealed in vials with fresh cod the sensor gave a detectable response after 8 hours at room temperature. This sensor is simple and works when exposed to raw fish samples warranting further considering for development, upscaling, and testing.

Mohr *et al.* developed a colorimetric sensor based on a pH indicator.[40] The pH indicator 2-fluoro-4-[4-(2-hydroxyethanesulfonyl)-phenylazo]-6-methoxyphenol (GJM-492) was used as it undergoes a color change from green to red upon deprotonation (Fig. 2c). The pH indicator was covalently immobilized onto microcrystalline cellulose, which was then dispersed into toluene and silicone (RTV615A), and then knife coated onto polyethylene terephthalate (PET). A top layer of silicone was added to prevent interferences by atmospheric pH changes and leaching of any chemicals (Fig. 2c). These sensors were exposed to ammonium chloride in aqueous sodium phosphate buffer (pH 8.4), yielding a defined amount of gaseous ammonia and observed a green to red color change (Fig. 2c). The sensor showed similar reactivity towards tryptamine, and higher responses to methylamine and dimethylamine due to their increased basicity and lipophilicity. Response of these sensors is very slow due to the additional layer of silicon, requiring 1.5 hours at a constant amine exposure to show a detectable color change. Overall, the sensor provides information on the total amount of amines, rather than selectively sensing one specific amine. Further testing was done using spoiled chicken and pork, showing a response when stored at room temperature after 1 and 2 days, respectively. Additionally, these sensors underwent cytotoxicity tests, an important step towards practical uses of these sensors in the food industry. It was found that colored cellulose particles as well as silicone embedded particles showed no cytotoxicity. These sensors show great promise due to their sensitivity to real-world meat spoilage and biocompatibility.

Colorimetric sensors are becoming more common, with some targeting specific amines,[76] some include a large range

of dyes in an array to target a variety of amines for a more complicated informational device.[41,76] These arrays have been developing towards discriminating between different types of amines (*e.g.*, triethylamine *vs.* isobutylamine *vs.* isopentylamine).[77] This is achieved with an array of membranes with different pH indicators and an analyzing portable instrument that can identify the exact red, green, and blue color changes before and after exposure to amines. Each specific amine will give a unique color pattern specific that the software can then identify. Of notable mention is a genipin-based colorimetric sensor, giving a colorless to blue color change in response to putrescine, cadaverine, tyramine, and histamine, as well as a response to uncooked decaying chicken.[78] This sensor, while highly selective and qualitative for biogenic amines, had a complicated preparation into alginate gel beads, which should be taken into consideration for large scale production.

2.2. Organic polymer-based colorimetric sensors

An emerging design strategy for amine sensing is to develop conjugated polymers (CPs) with a high electron affinity as to promote interactions with electron donating amines. This can be achieved through functionalizing CPs with electron-withdrawing groups to render the conjugated backbone electron deficient. Kwak *et al.* exploited this strategy using a nitrated polythiophene (NPTh) as the active layer in a colorimetric sensor (Fig. 3a).[42] The polythiophene provided a conjugated backbone that was rendered electron deficient through functionalizing with nitro groups. This nitrated CP was designed to form an intermolecular charge transfer complex with amines resulting in a color change of the organic film. The colorimetric device formation is like those mentioned previously, with an active layer supported by an inert substrate. Devices were fabricated by spin-coating films of NPTh from a THF solution onto glass and drying under vacuum at 50 °C for

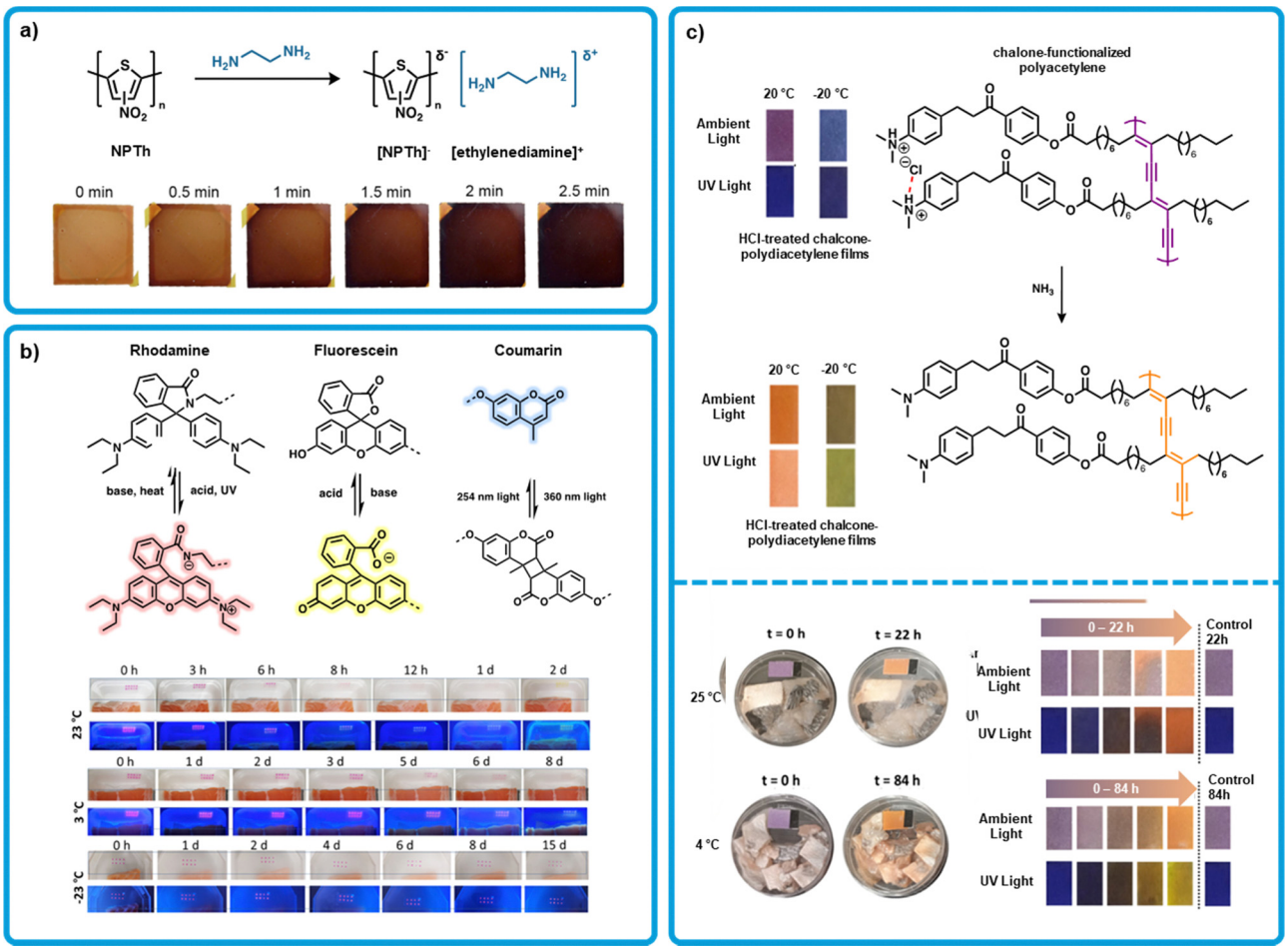

Fig. 3 Polymeric organic colorimetric amine sensors. (a) Formation of a charge transfer complex of NPTh and ethylenediamine. Inset: Modified images of colour change observed in spin-coated films of NPTh on glass over time upon ethylenediamine exposure with permission from Kwak *et al.*[42] (b) Mechanisms of the interaction of rhodamine, fluorescein, and coumarin upon exposure to acid, base, and/or UV light. Inset: Modified images of drop-cast, UV light pretreated sensor arrays upon exposure to salmon samples stored at different temperatures. Adapted with permission from H. Zhang, X. Wei, M. B. Chan-Park and M. Wang, *ACS Food Sci. Technol.*, 2022, **2**, 703–711. Copyright 2022 American Chemical Society.[68] (c) Top: Deprotonation of chalcone functionalized polydiacetylene after exposure to ammonia, inset: modified images of the resulting temperature-dependant colour change Jelinek *et al.*[69] Bottom: Modified images of chalcone functionalized polydiacetylene on filter paper upon exposure to rotting *Sparus Aurata* at 25 °C (Top) and 4 °C (Bottom) with permission from Jelinek *et al.*[69]

one hour. Polymer films were orange and upon exposure to ethylenediamine vapors turned near black (Fig. 3a). Optical spectra upon exposure to amines showed panchromatic absorption from 450 to 700 nm, giving rise to the black color. The rate of color change was faster for smaller amines that could diffuse more readily into the polymer film. The LOD was stated to be 5.6, 0.92, and 0.45 ppm for ethylenediamine, putrescine and cadaverine, respectively, indicating a sensitive sensor. Exposure of the sensor to decomposing beef, pork, and salmon resulted in the expected color change. It was assumed that the color change was due to cadaverine exposure, and the concentration was calculated to be at 242 ppm for beef, 177 ppm for pork, and 155 ppm for salmon after 3 days. The sensor was proven to detect BAs but has yet to be turned into a dosimeter to monitor rates of decomposition.

Wang *et al.* developed a series of polymers for use as multifunctional sensors using coumarin, rhodamine and fluorescein dyes (Fig. 3b).[68] The authors used the differing photophysical properties of these dyes to enable amine sensing. Polymers were synthesized with a methacrylate backbone and featuring either rhodamine or fluoresceine. All polymers were functionalized with coumarin. Rhodamine can be rendered base reactive when pretreated with acid or UV light, while fluoresceine is base reactive to start. When pretreated, rhodamine becomes a pink dye which can be quenched by base. The yellow color of fluoresceine is activated by base and deactivated by acid. Thus, these dyes work in tandem to create a pink to yellow color change on exposure to bases like BAs. Sensors were fabricated by preparing a 1 : 1 blend of the resulting polymers dissolved in ethanol and drop-casting onto PET substrates. Sensors were then irradiated with UV light (365 nm) to crosslink through the coumarin moieties, as well as activate the rhodamine into its pink, base reactive form. Crosslinking contributes to mechanical stability of films, thus making re-use of cross-linked sensors appealing. Treatment of activated sensors with ammonia lead to a sharp pink to yellow colour change, however at very low concentrations a colour change from pink to colourless was observed instead. This is attributed to the significantly higher sensitivity of activated rhodamine to base than fluoresceine. Upon exposure to other volatile amines (0.18 μmol in a 4.3 cm^3 cuvette; trimethylamine, triethylamine, morpholine) a pink to colourless colour change was observed, again highlighting the mis-matched sensitivity. Sensors showed no response to other common lab chemicals, such as methanol, ethyl acetate, chloroform, *etc.* Similar results were observed when sensors were exposed to spoiling salmon. A pink to colourless change was observed at room temperature within 6-8 hours, and a pale-yellow colour appearing after 24 hours and becoming obvious after 48. While an ideal sensor may require a better matched pair of sensing moieties to avoid the pink to colourless transition observed here, Wang *et al.* present a good method for increasing the magnitude of colour change by using 2 sensing moieties in tandem.

Jelinek *et al.* developed a sensor capable of sensing both amine vapor and temperature changes through thermochromism using chalcone functionalized polydiacetylene (Fig. 3c).[69] 10,12-Tricosadiynoic acid was functionalized with a chalcone moiety. The resulting monomer was drop-cast onto filter paper from chloroform and exposed to saturated HCl vapour, after which the film was photopolymerized using UV light (254 nm). The resulting sensors were then exposed to ammonia vapour at 20 °C, where a purple to orange colour change was observed, and −20 °C, where a blue to green colour change was observed. Alongside the colour change, a fluorescence enhancement was also noted at both temperatures. A LOD of 3 ppb was determined, based on a 1% fluorescence enhancement. Tests were then performed for detecting BAs produced by *Escherichia coli*, and a colour response was observed after 3 hours. Further tests were also performed using spoiled fish (*Sparus Aurata*), chicken, and beef. In all cases, a colour change was observed with 24 hours for samples left at room temperature. A fish sample left at 4 °C showed a significant response within 84 hours. Further, this sensor shows a time-dependent thermochromic response, turning from blue at −50 °C to purple at 20 °C to orange at 70 °C. A dual-action sensor like this one could be highly appealing as a food sensor, where both temperature fluctuations and amine off-gassing can indicate food is unsafe to eat.

3. Fluorescent sensors

Fluorescent sensors for amine detection are popular due their high sensitivity, low cost, and ease of operation when compared to electrochemical based sensors.[79–93] However, these sensors rely on either illumination with specific wavelengths of light (generally UV) to determine a color change in emission by eye or camera or *via* analysis with equipment, such as a fluorimeter, that can measure the emission profile of the sensing material to determine the response status. It is unlikely that a fluorimeter will be a common piece of equipment in households, however, it could be that the common household would adopt UV-light flashlights that can illuminate such fluorescent sensors to obtain a reading. Therefore, in terms of how easy it is to obtain a reading, a colorimetric sensor is advantageous over a fluorescent one, however, fluorescent sensors for BA detection exhibit low LODs, high sensitivity, and good selectivity and thus are still worth considering. To the best of our knowledge, there are no commercialized fluorescent sensors for food packaging at this time.

There are several potential sensing mechanisms when it comes to fluorescent sensors and can be first categorized as either ''turn off'' or ''turn on'', where a turn-off sensor is one where the emission intensity of the sensing probe decreases, alternatively, turn-on behavior sees emission-intensity increasing in response to stimuli.[43] In addition to change in emission intensity, a response can also be determined by a change in emission wavelength, thus exhibiting a color change in emissive light. How the fluorescent sensing materials see these types of responses can differ greatly, where aggregation,[44,86,94,95] charge transfer,[96–99] and acid–base reactions[100] have been used to achieve this.

Commercialization has not been achieved for fluorescent BA sensors, however, due to their excellent LODs they should be

Table 2 Summary of fluorescent BA sensors

Sensor	Change in emission	Sensing mechanism	Source of BAs	LOD	Film substrate/coating method	Ref.
PDI or PMI	"Turn-off"	Photoinduced electron transf.	Neat samples	0.1 mM (aniline)[ab]	Quartz/drop-casting	34
HPQ-Ac	"Turn-on"	Aminolysis – AIE	Saury fish (2 days)	20 ppm (ammonia)[c]	Filter paper/drop-casting	43
Benzannulated PDI	AIE switch	Ring opening – AIE switching	Fish	4.3 ppm (putrescine)	Glass & filter papers/drop-casting	109
BZCO	"Turn-on"	Aminolysis – ICT	Fish (4 days)	3.82 ppm (propylamine)	Filter paper/sip-coating	45
Cationic polymers	"Turn-off"	—	—	1.4 ppm (aniline)	Coated on interior of glass capillary	121
FITC, PPIX	Ratiometric emission colour change (red → green)	Nucleophilic attack	Shrimp (1 day)	5 ppm (ammonia)[a]	Electrospinning – nanofibrous membranes	125
TGH^{+}·PD	"Turn-on"	ICT	Chicken (28 hours)	2.04 ppb (ammonia)	Filter paper/dip-coating	127
COF-1-dye complexes	Colour change	N → B bond cleavage	—	0.1 ppm (ammonia)[b]	Aqueous dispersion	132

[a] No LOD is provided. Value given is the lowest reported to give an observable colour change. [b] Lowest reported solution-phase measurement. [c] Reported as the lowest concentration where fluorescence is visible to the naked eye.

considered. The current technologies are further off from their colorimetric counterparts, as many studies still rely on fluorescent sensors in solution form, which would be difficult to implement into food packaging directly. However, many of these systems have shown that they can form thin films *via* printing/coating methods or be functionalized on substrates directly and retain their sensing behavior. Therefore, this section will focus on fluorescent based BA sensors and their potential as thin film sensors and their commercialization potential. These sensors are summarized in Table 2.

3.1. Organic molecule-based fluorescence sensors

Valiyaveettil *et al.* developed a "turn-off" perylene diimide (PDI) and perylene monoimide (PMI) and based sensors using chromophores with 2-ethylhexyl side chains at the imide positions (Fig. 4a).[35] PDI derivatives have high extinction coefficients and elevated fluorescence quantum yields (close to unity) in the red,[101] this combined with their electron deficient nature allows them to interact and detect amines.[102] Here, solutions of PDI or PMI (0.1M) were combined with amine solutions of varying concentrations (0.1–1.0 M). PMI and PDI solutions both showed quenched PL in response to amine exposure, most significantly to dimethylaniline (>90%). Solution PL was quenched with other reference amine vapors such as butylamine, diisopropylamine, and triethylamine, as well as BAs including phenylethylamine, and putrescine. This quenching effect is theorized to be due to photoinduced electron transfer from the HOMO of the electron donating amines to the HOMO of photoexcited perylene derivative.[35] Notably, PMI consistently showed a greater PL quenching response than PDI. This is attributed to the lower lying HOMO of PMI (HOMO energy of PMI = −6.22 eV relative to PDI = −5.99 eV), which is more favorable for photoinduced electron transfer from the amines. Further, Valiyaveettil *et al.* investigated PL quenching in drop-cast films. Here, PDI solutions in THF were drop cast onto quartz plates and dried at 70 °C giving active films which were then exposed to amine vapors (0.5 mL of amine solution in 5 mL glass vial placed inside a 15 mL chamber with the sensor for 12 hours). PL quenching was observed with and PMI exhibiting the best response. This work showcases how PDIs and related molecules can be effectively used as amine sensors. It is thus important to note that a myriad of PDI based materials have been reported, notably PDIs with bulky groups,[89,103–106] to prevent aggregation, change color, and increase PL intensity, providing numerous opportunities for selective sensor development.

Tang *et al.* developed a "turn-on" amine sensor based on 2-(2-hydroxyphenyl)quinazolin-4(3*H*)-one (HPQ-Ac) (Fig. 4b).[44] Solid-state sensors were fabricated by drop-casting HPQ-Ac from dichloromethane (10 mM) onto filter paper. The films were not emissive under UV irradiation (365 nm) as determined by PL spectroscopy. After exposure to increasing ammonia vapour, a steady increase in light emission was observed. Above 20 ppm of ammonia fluorescence can be observed by the naked eye with the assistance of a portable UV lamp. This fluorogen was designed to exhibit aggregation-induced emission (AIE) properties *via* an excited state intramolecular proton transfer and restriction of molecular motion mechanisms thus blocking vibrational relaxation mechanisms.[107] Materials which demonstrate AIE have been previously shown to be advantageous for fluorescent sensors because they do not require dispersion in solution or in a matrix.[44] The phenoxyl-acetyl group of HPQ-Ac was used to prevent intramolecular hydrogen bond and block proton transfer and thus quench fluorescence.[108] Here, amines cleave the *o*-acetyl bond through an aminolysis reaction restoring intermolecular hydrogen bonding. This restriction of molecular motion allows for emission in the solid state (Fig. 4b). This bond cleavage renders the photoluminescence change of sensors fabricated from HPQ-Ac irreversible.

This sensor demonstrated a "turn-on" response to ammonia, hydrazine, and various alkyl amines (benzylamine, ethylamine, diethylamine, trimethylamine, and triethylamine). These vapors

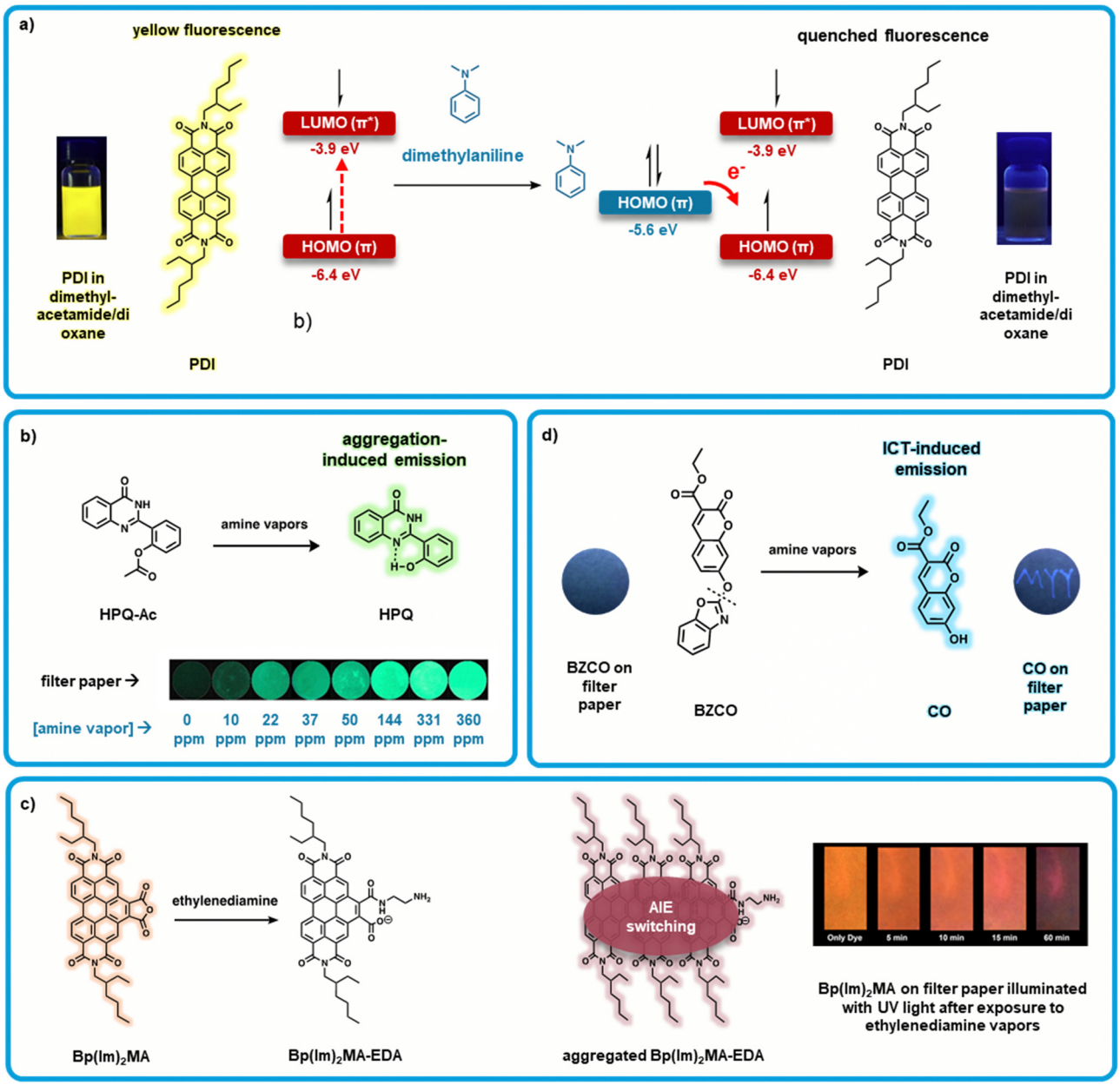

Fig. 4 Organic small molecule-based fluorometric amine sensors. (a) "Turn-off" PDI based sensors upon exposure to dimethylaniline resulting in quenched fluorescence due to electron transfer from the HOMO of dimethylaniline to the HOMO of PDI, inset: modified images of PDI in dimethylacetamide/dioxane before and after dimethylaniline exposure with permission from Valiyaveettil *et al.*[35] (b) Exposing HPQ-Ac to amine vapors produces HPQ, where HPQ aggregation-induced emission is observed due to intramolecular hydrogen bonding between the hydroxyl and quinazoline groups, inset: modified images showing the response of HPQ-Ac loaded filter papers to varying concentrations of amine vapor. Adapted with permission from M. Gao, S. Li, Y. Lin, Y. Geng, X. Ling, L. Wang, A. Qin and B. Z. Tang, *ACS Sens.*, 2016, **1**, 179–184. Copyright 2016 American Chemical Society.[44] (c) $Bp(Im)_2$-MA converts to $Bp(Im)_2$MA-EDA upon exposure to ethylenediamine (EDA), which then aggregate to induce AIE switching which both red-shifts and reduces the intensity of the emission wavelength. Inset: Modified image of $Bp(Im)_2$MA on filter paper when illuminated with UV light after exposing to EDA vapors over time. Adapted with permission from R. Roy, N. R. Sajeev, V. Sharma and A. L. Koner, *ACS Appl. Mater. Interfaces*, 2019, **11**, 47207–47217. Copyright 2019 American Chemical Society.[109] (d) BZCO is converted to CO *via* cleavage of the benzoxazoly unit by amines, inset: modified images showing response of BZCO loaded filter papers to a UV light before and after amine exposure spelling the letters "MYY", with permission from Hu *et al*[46].

could efficiently cleave the *o*-acetyl bond to generate an emissive HPQ product. Sensors did not light up on exposure to aromatic amines (aniline, and 2-methylaniline) and BAs (putrescine, cadaverine, and histamine) due to lower basicity and nucleophilicity of aromatic amines, and low vapor pressure of the BAs relative to the reference amines. This sensor was then tested with a sample of saury fish. After 2 days, the sensor began to fluoresce demonstrating a proof of concept.

Koner *et al.* further developed a sensor using the principles of AIE based on benzannulated derivative ($Bp(Im)_2$MA; Fig. 4c)

of 2-ethylhexyl PDI.[109] This sensor exhibits "AIE switching", where the emission wavelength is both decreased and red-shifted upon exposure to amine vapor. $Bp(Im)_2MA$ features an anhydride moiety which ring-opens forming to form a carboxylate ($Bp(Im)_2MA$-EDA) when exposed to ethylenediamine (EDA). This new compound exhibits AIE, detectably altering the emission characteristics. "Turn-on" probes which exhibit AIE are relatively common, but dual emissive fluorophores which switch from one mode to another are far less common.[110,111] Initial testing in solution found that only diamine or polyamine-containing reference amines and BAs (*e.g.* EDA, 1,3-diaminopropane, 1,4-diaminobutane, spermine and spermidine) lead to large change in absorbance and emission, while monoamino species showed very little change (*e.g. n*-butane, triethylamine, diethylamine, aniline, dimethylaniline). It is unclear whether selective detection of diamines and polyamines presents an advantage over other sensors; most BAs are diamines, so selectivity towards diamines may reduce false and erroneous readings due to the increased selectivity for diamines. This advantage will need to be weighed against the disadvantage of ignoring ammonia, a prevalent indicator of food spoilage.[112,113] These solution based sensors were transitioned to solid-state using two substrates: glass cover slips and filter paper, and were coated with thin films *via* drop-casting. Cover slip sensors showed a marked change from orange to red emission upon exposure to ethylenediamine. Filter-paper supported sensors showed a colour change as well as significant emission quenching that was time-dependent, while the glass cover slip sensors were found to be effective in detecting the decomposition of fish samples within a 48 hour exposure. While further development is needed to enable large-scale fabrication of sensing devices, this sensor shows an interesting use of a unique "AIE switching" mechanism and demonstrates the implementation of a diamine-selective sensor.

Hu *et al.* developed another "turn-on" sensor using coumarin functionalized with a benzoxazoly substituent (BZCO; Fig. 4d).[46] The "turn-on" effect of this sensor is explained by incorporation of the benzoxazoly substituent. This localizes the HOMO to the benzoxazole moiety, with the LUMO localized to the coumarin ring, as confirmed by density functional theory study. This effect disrupts internal charge transfer (ICT), and thus quenches fluorescence. Cleavage of the *o*-benzoxazole group results in formation of 7-hydroxy-2-oxo-2*H*-chromene-3-carboxylic acid ethyl ester (CO), and places both the HOMO and LUMO over the coumarin ring, thus restoring ICT and therefore fluorescence. Solid-state sensors were fabricated by soaking filter paper in CH_2Cl_2 solution (10 mM) of BZCO. A selection of amines (ammonia, hydrazine, primary and secondary amines) was shown to be capable of cleaving the benzoxazole substituent through an aminolysis reaction, restoring a strong fluorescence. Sensors did not show a significant response to tertiary amines, likely due to their lower basicity and nucleophilicity. A LOD of 3.82 ppm was determined for propylamine, demonstrating the high sensitivity of this sensor. When exposed to samples of spoiled fish, these sensors showed a response which was visible to the eye.

3.2. Organic polymer-based fluorescence sensors

Conjugated polymers are useful for fluorescence based rapid detection as they exhibit large signal amplification due to delocalization and rapid diffusion of excitons through the individual polymer chains, referred to as the molecular wire effect, or one point contact and multipoint response effect in solution and in thin films.[114–116] Post-polymerization ion exchange is a method to modify the conjugated polymers impacting optoelectronic properties,[117] charge transport,[118] hygroscopicity,[119] and electrostatic interactions with electrolytes.[120] Swager *et al.* developed a series of fluorescent cationic conjugated polymers with four different counter-anions (Fig. 5) to detect and differentiate between different amine vapors, denoted as PPymPH:Cl, PPymPh:DS, PPymPH:FTPB, and PPymPH:BF_4 depending on counter-anions.[121] Fluorescent active layer films were prepared by spin coating polymer solutions on glass substrates, then drying overnight in a vacuum at 60 °C. Films were cast from solvents trifluoroethanol (for PPymPH:Cl, and PPymPh:DS), acetone (PPymPH:FTPB), and DMSO (PPymPH:BF_4). For exposure to volatile amines, polymer films were coated on the inner wall of a glass capillary and the fluorescence was continuously monitored using a commercial FIDO sensor (FLIR Systems, Inc). This FIDO sensor allowed for recording of the fluorescence response to analyte vapors generated at specific concentrations with a gas generator. A series of amines were selected, each polymer was exposed, and the fluorescent response (quenching induced by amines) was recorded. These responses were found to be fully reversible in air. Each polymer composition gave differential responses to each amine, indicating a potential use and utility as a sensor array. An array was developed with the four polymers and exposed to 100 ppm of the seven selected amine vapors for 30 seconds. Detection limits were calculated for various amines, with the highest sensitivity found for aniline with a LOD of 1.4 ppm. Amine specific patterns were observed, and a quantitative view of the sensor array was developed by a linear discriminant analysis (LDA) performed on the data. LDA is a statistical analysis method that classifies analytes in predetermined classes, allowing to quantify the performance of a sensing array.[122] To further improve the mini-array, information on the kinetics of the responses were included, which has proven useful for the discrimination of analytes.[123,124] Incorporating quenching intensities measured at 15 seconds of exposure, 30 seconds of exposure, and 30 seconds post-exposure improved the

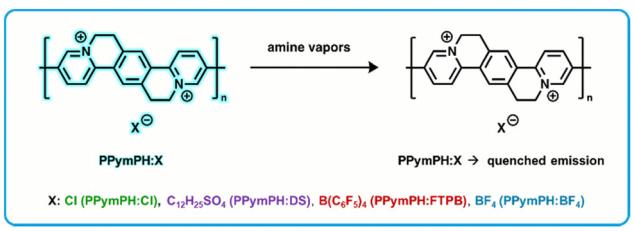

Fig. 5 PPymPh:X based "turn-off" fluorometric amine sensor exhibits analyte-induced emission quenching upon exposure to amine vapors.[121]

discriminating power to correctly classify 92% of the analytes. Aniline, butylamine, and pyridine were consistently correctly identified while diisopropylamine, diisopropylethylamine and triethylamine had some misidentification (as expected from their overlap and clustering). These three amines were still correctly identified 76% of the time.

Zhang *et al.* developed a dual-emissive ratiometric amine sensor by grafting emissive organic molecules to cellulose acetate, a polymer derived from naturally occurring cellulose.[125] One of two fluorophores, fluorescein isothiocyanate (FITC) or protoporphyrin IX (PpIX), were covalently tethered to cellulose acetate (Fig. 6a). The two grafted polymers were blended in a ratio of 5 : 1 FTIC : PpIX. PpIX is a red emitter and not amine reactive, and thus is used as an internal standard. Upon exposure to amine vapor, FITC becomes a strong green emitter, and is thus the active sensing moiety. Due to the excess of FITC, green emission becomes dominant upon amine exposure, making green emission an indicator of food spoilage. The solution processability of cellulose acetate was not hindered by the incorporation of fluorophores and the authors demonstrate a variety of techniques for possible sensor fabrication, including pattern-printing and electrospinning, to form nanofibrous membranes. Initial testing of the nanofibrous membranes upon exposure to ammonia vapor indicated the dual-emissive sensors were capable of quantitatively detecting ammonia using the ratio of emission from FITC and PpIX. No detection limits were calculated, but a response was observed at a 5 ppm ammonia concentration, the lowest tested. Further testing showed a strong response to other reference amines (diethylamine, pyrrolidine, benzylamine) as well as a selection of BAs (putrescine, histamine). Notably, these sensors can be reversible; the emission intensity of FITC could be fully quenched by heating, after which re-exposure to ammonia re-activated emission. When applied towards the detection of spoilage of shrimp, sensors successfully identified shrimp which was unsafe to eat based on the total volatile basic nitrogen (TVB-N).[112,126] The authors also considered colony forming units (CFU) in the food samples, but highlight that there is no standard for what CFU value is considered unsafe. It should be similarly noted that safe TVB-N levels tend to be similarly variable, and are only extensively explored for fish.[112] This ratiometric system is extremely promising – especially for solution processability and its ability to quantify ammonia exposure.

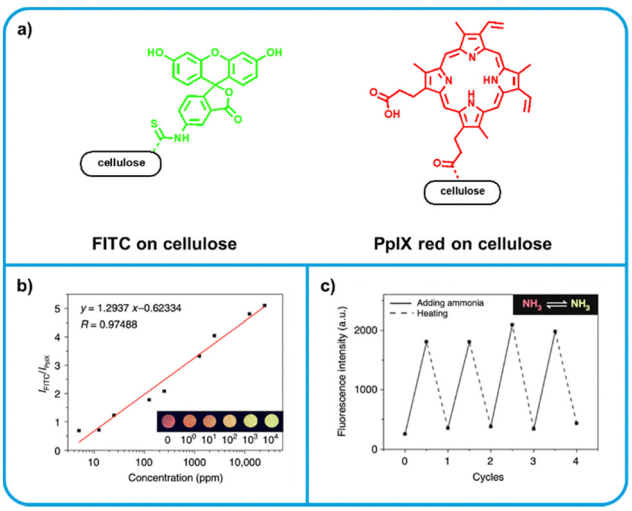

Fig. 6 Dye-tethered cellulose acetate based ratiometreic amine sensor. (a) Structures of dye components. Left: FITC becomes a strong green emitter upon exposure to amine vapour. Right: PpIX is unreactive towards amines, thus its red emission can be used as an internal standard. (b) The logarithmic relationship between concentration of ammonia analyte and the ratio of FITC to PpIX emission intensity. This relationship allows for quantitative determination of ammonia concentration. (c) Reversibility of sensor turn-on upon heating. Adapted with permission from Zhang *et al.*[125]

3.3. Covalent organic framework based fluorescence sensors

A "turn-on" sensor based on an ionic covalent organic framework (iCOF) using triamino-guanidinium hydrochloride (TGH^+) and phenanthroline-2,9-dicarbaldehyde (PD) was developed by Trabolsi *et al.* and is one of the most recent BA sensors reported (Fig. 7).[127] Fluorescence in this iCOF system is attributed to ICT from the PD to the TGH^+ moiety. Similar ICT probes are known to exhibit changes in fluorescence upon binding with analytes.[128] This fluorescence effect, combined with the Lewis acidity of TGH^+·PD made this system highly attractive for applications in amine sensing. Initial tests with a dispersion of TGH^+·PD in water found a detection limit of 1.2×10^{-7} M for ammonia, comparable to other high sensitivity chemosensors.[129–131] Further testing was carried out exposing these dispersions to saturated ammonia vapors for 10 seconds, after which a tripling in fluorescence intensity was observed. This effect was also found to be highly reversible which is a parameter ideal for reusable BA sensors. When these dispersions were exposed to raw chicken at room temperature, a significant increase in fluorescence intensity was observed over time. Notably, these sensors show a high degree of selectivity towards ammonia and other small amine vapors with little to no detectable fluorescence changes observed upon exposure to other, bulkier amines. While the sensitivity of these dispersion sensors is appealing, it is unclear how this system can be implemented in food packaging as a BA sensor. Alternatively, solid-state sensors were fabricated by dipping filter papers in aqueous dispersions of TGH^+·PD and then were then placed in a container with raw chicken, upon exposure to amine vapors a color change was observed. These solid-state sensors are arguably more viable to implement in food packaging, however, it is unclear if the sensitivity parameters are appropriate for rotting chicken specifically.

Ma *et al.* developed a series of COF based amine sensors using COF-1, a phenyl diboronic acid-based COF first reported by Yaghi *et al.*[132,133] While COF-1 is non-emissive, the authors found that incorporating emissive pyridine-containing dyes a series of emissive dye-COF hybrids could be developed (Fig. 8a). Specifically, upon mixing solid 2,4,6-triphenylboroxin, a model for COF-1, and *N*,*N*-diphenyl-4-(pyridin-4-yl)aniline (TPA-Py) a large bathochromic shift in emissive wavelength is observed (110 nm). This behaviour is indicative the formation of the

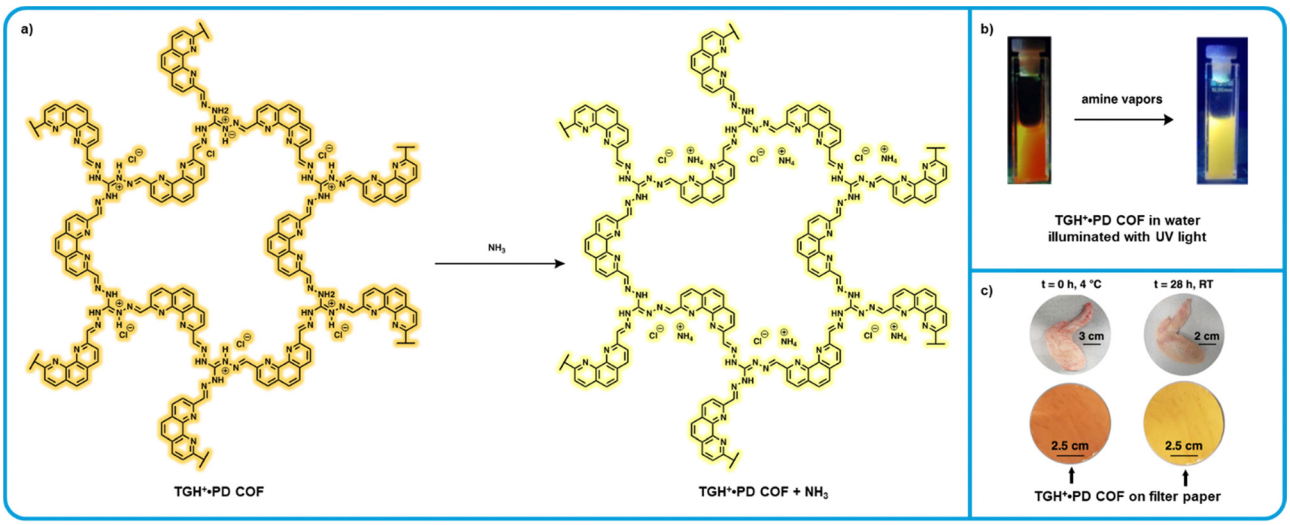

Fig. 7 TGH^+·PD based "turn-on" fluorometric amine sensor. (a) Mechanism for the interaction of TGH^+·PD with ammonia. (b) Modified images showing the resulting change in photoluminescence of TGH^+·PD water dispersions from Trabolsi *et al.* (c) Modified images showing the color of TGH^+·PD on filter paper after exposure to fresh and rotting chicken wit permission from Trabolsi *et al.*[127]

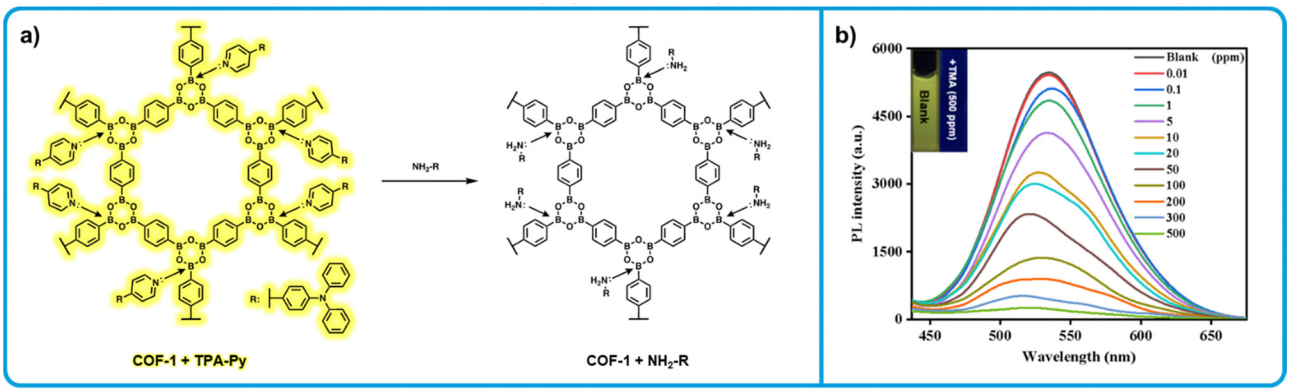

Fig. 8 COF-1 based "turn-off" fluorometric amine sensors. (a) Mechanism for the interaction of COF-1-pyridine dye-based sensors with aliphatic amines resulting in a decrease in emission of the COF-1-dye emission. (b) Emission decrease of COF-1-dye upon exposure to increasing concentrations of trimethylamine. Adapted with permission from Y. Sun, B. Zhang, C. Zhang, H. Lu, Y. Yang, B. Han, F. Dong, J. Lv, S. Zhang, Z. Li, Z. Lei and H. Ma, *ACS Appl. Mater. Interfaces*, 2023, **15**, 4569–4579. Copyright 2023 American Chemical Society.[133]

N → B allows the electron poor B to act as a withdrawing group, altering the emission wavelength of the dye. Absorption data makes clear that a charge transfer occurs during N → B bond formation. When similar complexes were prepared from COF-1 and a series of different pyridine containing dyes, similar bathochromic shifts were observed, ranging from 40–170 nm. The authors show that due to the sensitivity of N → B to electron donating groups, such as aliphatic amines, these complexes can effectively function as amine sensors. In aqueous dispersions, significant fluorescence quenching was observed upon addition of trimethylamine due to the displacement of the pyridine-containing dye. Further, all COF-1 dye complexes were exposed to 10 ppm of trimethylamine, triethylamine, tetramethylenediamine, diethanolamine and ammonia, with all complexes showing significant fluorescence change to each. Aniline and *cis*-1-amino-9-octadecene were also tested, with little response to either. This is attributed to the lower electron donating ability of aniline. For *cis*-1-amino-9-octadecene, it is likely the long, bulky chain disrupts exchange with the pyridine dyes, similar to what is observed with bulkier amines in Tripoli *et al.*[127] The authors did not investigate the solid-state fluorescence change upon exposure to amine vapours, but similar results are likely due to the low amine concentrations required to show a response in dispersion. While no viable method of sensor fabrication is presented, COF-1 dye hybrids present a simple method to develop a series of tunable amine sensors.

4. Electrochemical sensors

Electrochemical sensors, like fluorescent sensors, are highly sensitive and generally exhibit low LODs. However, they are

more difficult to develop as sensors for food packaging than their colorimetric and fluorescent sensor counterparts due to requiring electrodes and a power source. What is advantageous about electrochemical sensors is their potential to be made reusable due to non-destructive sensing modes that are reversible, therefore, they remain economical regardless of a high production cost. Furthermore, these sensors have the potential to be calibrated for various types of foods, so one sensor would not have to be limited to one specific food product, which is significant considering the different BA profiles that occur in various food types.[24–26]

Many different types of device designs can be employed to realize electrochemical sensors, some of which include radio frequency identification (RFID) tags,[134,135] chemiresistors,[136,137] and transistors.[138,139] In the case of a RFID tag, the power source can be provided wirelessly by a cellular device, and therefore are appealing as one time use sensors in food packaging.[134,135] Despite the many advantages of RFID technology, to our knowledge it has been seldom applied towards BA food sensors,[140,141] and therefore further work should be done to develop this technology. Chemiresistors and transistors require a power source such as a battery, and therefore are more likely to be developed as reusable devices. In terms of sensing mechanisms, electrochemical devices contain either hole or electron transporting materials, therefore, upon applied stimuli a change in current is measured as a result of changes to the bulk material chemical and/or physical properties. Organic π-conjugated compounds can be used as the sensing material in these devices as they can be rendered hole or electron transporting as thin films.[142–145] BA sensing using organic materials in electrochemical devices utilizes that BAs contain basic amine sites that are capable of deprotonating acidic sites on organic π-conjugated compounds such that the electronic structure is altered, that promote intermolecular interactions which in turn disrupts molecular order and as a result charge transport, and that impart chemical changes that affect π-conjugation of the organic material, where all of these scenarios serve to alter the current measured from the device.

Fully printed flexible electronic devices have been under development in recent years, thus all organic electrochemical sensors hold potential for large scale manufacturing *via* printing methods.[146–148] Additionally, many different types of RFID tags are currently mass produced and can be very cost effective, making RFID based sensors very promising candidates for food sensors as the final device can be easily produced by depositing/printing a small amount of the organic sensing material on a pre-made tag. For chemiresistive sensors, films can be printed and electrodes deposited on top, making this design simple and easy to fabricate. For transistors, the potential for commercialization depends on the device design, where organic field effect transistors (OFETs), for example, have many components to consider and would be more challenging to mass manufacture, but have proven to be highly sensitive and have low LODs.[139,149,150] The electrochemical sensors covered here are summarized in Table 3.

4.1. RFID based sensors

RFID is a highly attractive technology for use as BA gas sensors as they can operate using a cellular device as the power source, as well as they are versatile in terms of form, fabrication and function.[134,135] Many RFID gas sensors are fabricated by the incorporation of a sensing region in contact with the antenna of the RFID tag.[135,140,151] This region serves to alter the capacitance or resistance (or in some cases both) of the circuit in response to a chemical and/or physical change to the sensing material. This change can be detected wirelessly using an RFID reader, thus enabling a readout.

Yu *et al.* developed a ''turn-on'' sensor capable of amine detection using an iron(III) *p*-toluenesulfonate hexahydrate-doped, nanostructured polyaniline (PTS-PAni) sensitizing layer.[140] PTS-PAni is reduced from its emeraldine salt form to its emeraldine

Table 3 Summary of electrochemical BA sensors

Sensor	Device type	Sensing mechanism	Source of BAs	LOD	Device fabrication	Ref.
PTS-PAni	RFID	Reduction (salt form to base form)	Pork, beef, chicken and fish (20 hours)	5 ppm (ammonia)	Inkjet printing onto a gold NFC coil	140
f-SWCNT	Chemiresistor	Formation of charge complex	—	40 ppm (ammonia, trimethylamine)	Drop-cast suspension. Thermally evaporated electrodes	35
TFMK-P3HT-CNT	Chemiresistor	Nucleophilic attack	—	—(Decreased relative to p-CNT)	Drop-cast suspension. Thermally evaporated electrodes	158
P3HT	Chemiresistor	Formation of charge complex	Tilapia, beltfish and mackerel (24 hours)	100 ppb (ammonia)[a]	Spin-coated active layer. Colloid lithography for porous electrode.	159
DPPT-TT	OFET	Ion formation → decrease in current	—	0.025ppb (butylamine)	Bottom-gate bottom-contact architecture. See above for details	145
pDPPCOOH-BT	OFET	Acid/base	Neat (putrescine; rapid)	10 ppb (ammonia)	Bottom-gate bottom-contact architecture. See above for details.	146
P3CPT	Electrolyte-gated OTFT	Acid/Base	Neat (histamine, putrescine, tyramine, histidine; rapid)	1.6 mM (histamine)[b]	Side-gate architecture. See above for details.	167

[a] No LOD is provided. Value given is the lowest reported to give a response. [b] In aqueous electrolyte solution.

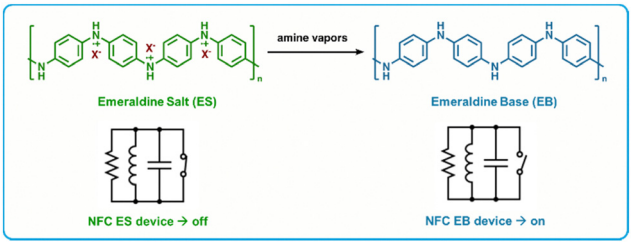

Fig. 9 PTS-PAni based RFID amine sensors. Top: Chemical change of PTS-PAni upon exposure to amine vapors showing the transition from the Emeraldine Salt form to the Emeraldine Base form. Bottom: State change for NFC tags caused by the increase in resistance upon conversion to the Emeraldine Base form. Adapted with permission from Z. Ma, P. Chen, W. Cheng, K. Yan, L. Pan, Y. Shi and G. Yu, *Nano Lett.*, 2018, **18**, 4570–4575. Copyright 2018 American Chemical Society.[140]

base form upon exposure to amines, which increases the resistance of the polyaniline film and switches the device from "off" to "on" (Fig. 9). These devices were fabricated by printing "dots" of PTS-PAni onto the gold coil of a RFID tag, which is a fabrication method that can be translated into large scale manufacturing easily. A two-fold increase in resistance was recorded in response to ammonia (5 ppm) as well as to cadaverine or putrescine (40 ppm). These sensors were highly selective for amines alone, as minimal response was recorded for other volatile organic analytes including methanol, dichloromethane, acetaldehyde, *n*-hexane and chloroform. Additionally, when exposed to samples of pork, beef, chicken, and fish left at 30 °C for 20 hours, the sensors switched to "on" by inducing resistance in the circuit. Importantly, the sensor's sensitivity towards BAs is large enough to be detectable by a smartphone's near-field communication (NFC) transponder, which enables accessibility to the public.

4.2. Chemiresistive sensors

Conductive organic materials such as carbon nanotubes have gained interest over the last 30 years due to their outstanding electrical, thermal, and mechanical properties and high aspect ratio.[152–155] They have been used as the sensing component in chemiresistive sensors for BA detection, as exposure to BAs can cause chemical and/or physical changes to the bulk material that then alters their electronic configuration and in turn causes changes to conductivity when in a device.[156–161] Towards this, Pucci *et al.* developed a CNT with a functional a perfluorophenyl-carboxylic acid moiety for amine sensing *via* formation of a charge complex with amines (Fig. 10).[36]

A sensor array was fabricated by thermally evaporating gold electrodes on glass slides and then drop-casting suspensions of carbon nanotubes functionalized with perfluorophenyl carboxylic acids (f-SWCNTs). Using an applied field of 0.1 V, the conductivity of this array was determined, and in this case the conductance (G = current/voltage) was directly proportional to the current. The normalized conductance ($\Delta G/G_0 = (G_0 - G)/G_0$) was also determined where G_0 represents conductance before exposure to any amines, and G represents conductance achieved during exposure to BAs. These devices exhibit a decrease in

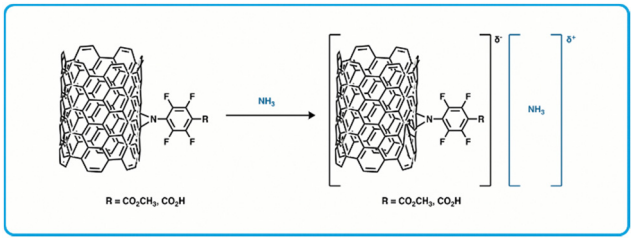

Fig. 10 Diagram of chemiresistor sensing materials using a perfluorophenyl carboxylic acid functionalized SWCNT and the formation of a charge complex with ammonia.[36]

conductance when exposed to specific amines, giving a positive $\Delta G/G_0$ value. This work showed a promising chemiresistive sensor for detecting low concentrations (40 ppm) of gaseous ammonia or trimethylamine (TMA). The sensors were highly selective towards ammonia and TMA, having little change to G_0 ($\sim$0.1%) when exposed to large concentrations (200 ppm) of alternate volatile organic compounds like tetrahydrofuran, hexane, ethyl acetate, ethanol, acetonitrile, and chloroform. While there was mention of detecting spoilage in seafood using these sensors, no additional efforts for food spoilage testing were made. However, considering this sensor exhibited a high sensitivity to specific amines and because they can be modified further to tune their performance, they warrant further investigation in terms of material modification for ideal parameters and fabrication optimization.

Koo *et al.* developed a CNT-polymer composite sensor using trifluoromethyl ketone functionalized poly(3-hexylthiophene) (TFMK-P3HT; Fig. 11).[162] The use of conjugated polymers is desirable, since their use has increased selectivity in CNT based sensors owing to their strong intermolecular interactions with CNTs and their ability to interact with amines *via* various functional groups. In this work, functionalization of P3HT polymers using trifluoromethyl moieties was done to incorporate electrophilic sites that are chemically reactive towards nucleophilic amines. Devices were fabricated by drop casting a blend of a polymer solution and CNT suspension (1 : 1 wt%) in $CHCl_3$ on glass substrates followed by thermal deposition of gold source–drain electrodes. TFMK-P3HT/CNT detected and showed a larger increase in resistance upon exposure to triethylamine, diethylamine or ethylamine, relative to P3HT/CNT sensors (4.36 times, 2.65 times, and 3.00 times, respectively). Furthermore, these sensors showed negligible sensitivity to a series of alcohols.[162]

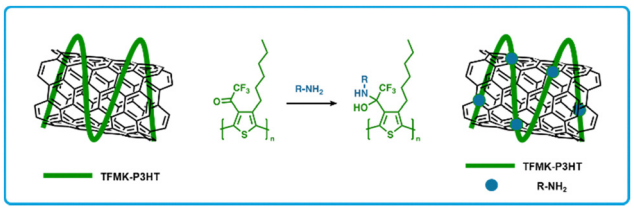

Fig. 11 Diagram of TFMK-P3HT/CNT chemiresistors and the resulting addition reaction of amines to the trifluoromethyl ketone unit on TFMK-P3HT/CNT. Modified from Koo *et al* with permission in ref. 162

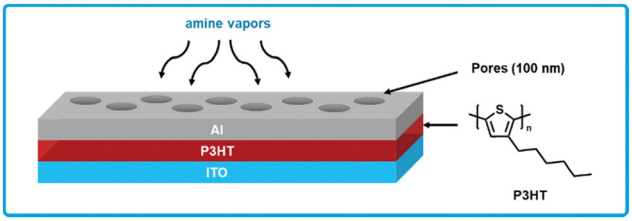

Fig. 12 P3HT based chemiresistive biogenic amine sensor. Cross-section showing the sandwich architecture with an ITO bottom electrode, P3HT active layer, and porous aluminum top electrode. Adapted with permission from L. Y. Chang, M. Y. Chuang, H. W. Zan, H. F. Meng, C. J. Lu, P. H. Yeh and J. N. Chen, *ACS Sens.*, 2017, **2**, 531–539. Copyright 2017 American Chemical Society.[163]

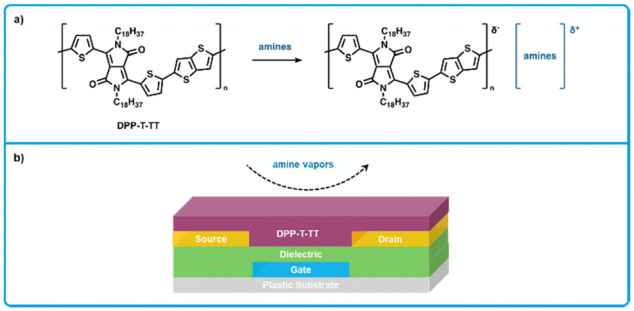

Fig. 13 DPPT-TT based OFET sensors for biogenic amines. (a) Mechanism for the interaction of DPPT-TT polymers and amine analytes. (b) Cross section showing the bottom-gate bottom-contact architecture used for fabrication of amine sensors. Adapted with permission from Persaud *et al.*[13,149]

Chen *et al.* developed a poly(3-hexylthiophene) (P3HT) based chemiresistive amine sensor (Fig. 12).[163] P3HT is a ubiquitous polymer in organic electronics due to its high performance as an organic hole transporting material paired with good solubility in common organic solvents and processability for device fabrication.[164] Sensors using P3HT were fabricated by spin-coating P3HT from a solution of chlorobenzene on top of a layer of indium tin oxide, which serves as the bottom electrode.[163] Polystyrene nano-spheres are then blade-coated on top of the P3HT, which serve as a shadow mask such that aluminum can be patterned on top using thermal evaporation. Additionally, the pores created by the nano-spheres allow amine vapor to diffuse through the aluminum top electrode to the P3HT active layer. Sensors response was tested on exposure to a series of reference amines (ammonia, dimethylamine, trimethylamine) ranging from 100 ppb to 1 ppm, where in each case the sensors responded to all amines at all concentrations tested. While no LOD is calculated, an 8% response was observed to 100 ppb of ammonia, implying the 1% response LOD is less than 100 ppb. Sensor response was reversible in nature, when the amine analytes were removed from the sensor the resistance gradually decreased to the original level. For tests with rotting fish, authors were able to detect BA vapors and convert the response into an effective ammonia concentration, which the authors demonstrate is linearly correlated to TVB-N, thus allowing for quantification of TVB-N. The simple fabrication of these sensors using commercially available materials combined with their low LOD and quantitative amine response makes these sensors highly appealing for further investigation into testing with real food and large-scale fabrication methods.

4.3. OFET based sensors

Organic field-effect transistors (OFETs) have a long-established history as gas sensors,[138,139,165,166] which can be attributed to their simple and inexpensive fabrication as well as their sensitivity and selectivity. Additionally, due to the multitude of parameters which can be measured from OFET devices, so-called "fingerprint" responses can be used to detect and identify target analytes, meaning analytes exhibit a unique response current.[166] While OFETs are of interest for applications as food sensors, these devices can suffer from high driving voltages, therefore, the devices considered for BA sensors should require low voltages such that a common battery can power them.[149,166,167]

Persaud *et al.* developed an OFET for the detection of amines using a diketopyrrolopyrrole-thiophene thienothiophene polymer (DPPT-TT) as a hole transporting active layer (Fig. 13) that required a low operating voltage of −3 V.[149,168,169] Upon exposure to amines, DPPT-TT forms ionic species, leading to a decrease in current across the OFET, which functions as the sensing response. The devices were fabricated by first thermally evaporating an aluminum gate electrode on a flexible polyethylene naphthalate substrate to yield a 50 nm film, followed by spin coating a high-*k* dielectric poly(vinylidenefluoride-trifluoroethylene-chlorofluoroethylene) on top of the gate followed by a low-*k* dielectric poly(methyl methacrylate) layer, and then gold source and drain electrodes were thermally evaporated directly on the dielectric. Following this, devices were then soaked in a solution of pentafluorobenzenethiol (PFBT) in ethanol (5 mM) to maximize charge injection from the top OSC layer, as PFBT chemisorbs to the gold electrode surfaces which increases the work function and thereby reduces the energy barrier for charge transfer.[170] Finally, DPPT-TT was spin-coated on top from 1,2 dichlorobenzene as the hole transporting layer (Fig. 13b). These devices were found to be highly sensitive to amines; showing a measurable decrease in current at sub ppm concentrations for all evaluated amines (ammonia, primary, secondary and tertiary). Specifically, the LOD for ammonia, butylamine, dibutylamine was measured at 2.17 ppb, 0.056 ppb, and 0.025 ppb, respectively. Importantly, these OFETs are capable of operation at a gate voltage of −3 V, which is considerably lower than many competing OFET amine sensors.[171] Previous work in the Persaud group has also demonstrated the use the solution-processed electrodes from a silver nanoparticle ink in low-voltage OFETs.[168] Therefore, these highly responsive, low-voltage OFET sensors could be developed further to realize applications in smart-food packaging owing to the previously demonstrated fully solution-processed fabrication thereby allowing viable large-scale production, and due to their low driving voltages, they could be powered by batteries or solar cells.

Zhang *et al.* developed a thin-film OFET ammonia sensor using a diketopyrrolopyrrole-bithiophene polymer as the

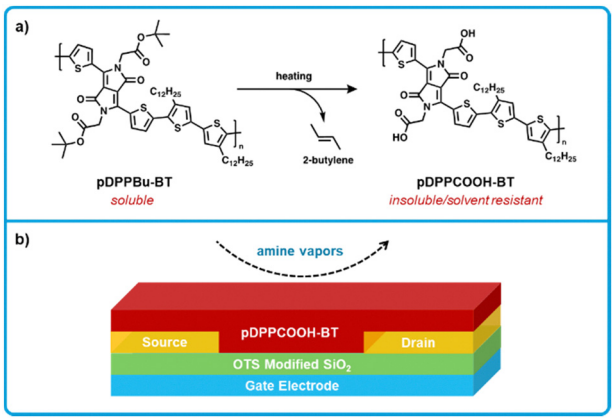

Fig. 14 pDPPCOOH-BT based OFET sensors for biogenic amines. (a) Thermal cleaving of pDPPBu-BT to form pDPPCOOH-BT. pDPPBu-BT a soluble form used to process the polymer before thermal cleaving forms the amine reactive form pDPPCOOH-BT. (b) Cross-section showing the bottom-gate bottom-contact architecture used for fabrication of amine sensors. Adapted with permission from Y. Yang, G. Zhang, H. Luo, J. Yao, Z. Liu and D. Zhang, *ACS Appl. Mater. Interfaces*, 2016, **8**, 3635–3643. Copyright 2016 American Chemical Society.[150]

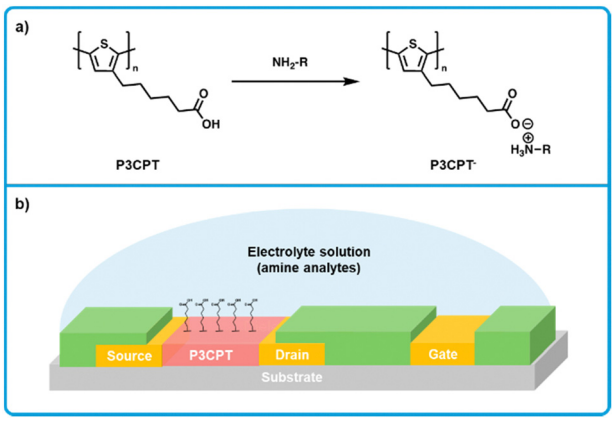

Fig. 15 P3CPT based electrolyte-gated OTFT sensor for biogenic amines. (a) Mechanism for the interaction of P3CPT polymers and amine analytes showing a deprotonation of P3CPT. (b) Cross section showing the side-gate architecture used for the fabrication of OTFT sensors. Modified with permission from Minami *et al.*[172]

charge transporting and sensing material, where *t*-butoxy groups were installed on the polymer (pDPPBu-BT) to yield solubility for solution processing, but were thermally cleaved post film formation to give carboxylic acids (pDPPCOOH-BT; Fig. 14).[150] OFETs were fabricated by using premade n-type Si wafers as the gate electrode with a SiO_2 dielectric on top. Gold source–drain electrodes were deposited on top of the dielectric and patterned using photolithography, as well as functionalized with a *n*-octadecyltrichlorosilane monolayer to modify the electrode surface and work function. Finally, pDPPBu-BT was spin-coated on top from 1,2 dichlorobenzene. Films were then thermally annealed under vacuum at various temperatures, annealing at 240 °C and above cleaves the *t*-butoxy groups to yield pDPPCOOH-BT (Fig. 14b). In terms of sensing, a reduction in on-current of the device was detectable when exposed to gas concentrations as low as 10 ppb for ammonia, where other volatile reference amines (triethylamine, piperidine) and BAs (putrescine) show similar reductions in on-current. It was then determined that the anionic species (carboxylates) generated from the deprotonation of pDPPCOOH-BT by amines leads to the generation of charge traps that serve to decrease current. This work exhibited low LODS and exhibited fast response times; however, more work is needed to translate this system to function on flexible substrates if the intention is to incorporate into food packaging. On the other hand, the use of premade silicon based wafers as the gate and dielectric reduce the number of fabrication steps and could be used to make a portable handheld device, especially considering the fast response times of this sensor on the order of a few seconds.

Minami *et al.* developed a electrolyte-gated thin-film transistor based on poly(3-[5-carboxypentyl]thiophene-2,5-diyl) (P3CPT; Fig. 15a),[172] where P3CPT was first reported for use in an organic thin-film transistor (OTFT) by Berggren *et al.*[173] In this work, transistors were fabricated with a side-gate structure (Fig. 15b).[172] Transistors were fabricated with a side-gate structure. Gold source–drain-gate electrodes were thermally evaporated onto glass substrates. A perfluoropolymer (Cytop) was then spin-coated on top of the electrodes and patterned using oxygen plasma etching to create hydrophobic banks that isolate the electrodes. P3CPT was then drop-cast from DMSO between the source and drain electrodes, and thermally annealed under an N_2 atmosphere. Finally, electrolyte solutions were dropped on top of the transistor (Fig. 15b). In terms of a sensing mechanism, when P3CPT is deprotonated, both channel conductivity and drain current decreases. This effect enables a dependence of drain current on electrolyte pH, where at high pH drain current is low and at low pH drain current is high. When the electrolyte solution (buffered at a pH of 5.5) was titrated with histamine, an increase in drain current was observed, where the LOD for histamine was estimated at 1.6 mM in in aqueous solution. Other BAs were tested (putrescine, tyramine, histidine), but did not react as strongly. Reference monoamines (methylamine, dimethylamine, trimethylamine) were also tested and gave very weak responses. While this work holds promise for detecting amines in aqueous solutions, more work is needed to explore other similar systems that can sense a broader range of BAs.

Conclusion and future outlook

Organic conjugated materials as the active component in optical (colorimetric and fluorescence-based) and electrochemical (RFID, chemiresistive, and OFET based) in amine sensors have been highlighted. Optical sensors feature an organic material which experiences some change in electronic structure upon amine exposure, leading to a change in color or photoluminescence. These sensors are simple to produce; the organic active layers are simply immobilized onto a support, such as cellulose paper or PET, yielding the completed sensor. This design lends itself toward production *via* roll-to-roll printing, making

large-scale production economical while minimizing adverse health and environmental effects when processed from non-toxic solvents.[67] Fluorometric sensors have been found to show higher selectivity than colorimetric sensors, but require irradiation with UV light before the sensing effect becomes obvious. Electrochemical sensors have been shown to be more sensitive and selective than optical sensors but are generally much more complex in design. RFID based sensors are a highly advantageous type of electrochemical sensor, as they can operate by use of a smart phone, are simple to use, and can be produced by performing a simple modification to commercially produced NFC tags. However, these sensors do not show the high sensitivity afforded by other electrochemical sensors. While OFET and chemiresistive sensors are capable of very high sensitivity, their complex design makes fabrication more challenging and costly, thus their integration into food packaging is less obvious. However, these devices can be non-trivial to produce as well be rendered reusable, making them appealing to produce as a more sophisticated device sold separately from food itself.

While it is clear that the active sensing platforms needed for BA food sensors are being developed, there are a number of questions which must be addressed before these sensors can be commercialized. First, while it is promising that many sensors are tested with and respond to rotting meat samples, these tests are generally performed with a lack of control. Additionally, there is no well recognized standard for at what threshold of amines these sensors should trigger. It is within reason to imagine these sensors triggering too early, which could lead to the wastage of food, or too late, which could cause illness. Selectivity is another question which must be addressed. It is well established that different protein sources release different BA profiles,[24–26] raising questions about whether sensors are applicable for different proteins. Absolute measures of food quality and safety, such as TVB-N or colony forming units follow this pattern and significantly vary across species.[112] Cross-disciplinary collaboration is likely required to answer these questions and establish exactly when different foods become unsafe and whether a unified metric for all foods is possible.

The final design of an ideal BA sensor must also be considered, where the sensing component of a BA sensor is only one aspect of the many components that can make up these devices. For example, in a large-scale application like incorporation into packaging, a single-use biodegradable sensor is best. This makes paper substrates or those based on cellulose highly appealing. For home use, where a consumer might apply the sensor, a more durable, multi-use sensor is more logical, where plastic or even more rigid substrates could be used. Further, encapsulation by a gas-permeable barrier layer may be necessary to reduce the contamination of the food products with the sensing materials. Additionally, the materials must be rendered non-toxic in the event they do come in contact with the products. This raises further questions concerning the effects of these layers on sensitivity and selectivity, as well as sensor lifetime. Finally, sensors must be easily readable and understandable. If the end user cannot accurately and reliably read the sensor, it is rendered useless or harmful in the event of a false reading.

BA sensors using organic sensing materials are rapidly advancing to meet the metrics necessary for commercialization. This leads to a new problem to address: moving from promising academic curiosities to capable real-world devices. This move will require the collaboration of bioengineers, chemists, materials scientists, and more to produce safe, reliable and inexpensive sensors for mass production.

Conflicts of interest

There are no conflicts to declare.

Acknowledgements

This work was supported by the NSERC Green Electronics Network (GreEN) (NETGP 508526-17).

References

1 United Nations Environment Programme, Food Waste Index Report 2021, United Nations Environment Programme, Nairobi, 2021.
2 W. H. Organization, *WHO estimates of the global burden of foodborne diseases: foodborne disease burden epidemiology reference group 2007-2015*, World Health Organization, Geneva, 2015.
3 T. A. McMeekin, *Emerging Infect. Dis.*, 1997, **3**, 541–549.
4 E. Balbinot-Alfaro, D. V. Craveiro, K. O. Lima, H. L. G. Costa, D. R. Lopes and C. Prentice, *Food Eng. Rev.*, 2019, **11**, 235–244.
5 L. Manjakkal, D. Szwagierczak and R. Dahiya, *Prog. Mater. Sci.*, 2020, **109**, 100635.
6 M. Alizadeh-Sani, E. Mohammadian, J. W. Rhim and S. M. Jafari, *Trends Food Sci. Technol.*, 2020, **105**, 93–144.
7 E. Kress-Rogers, *Trends Food Sci. Technol.*, 1991, **2**, 320–324.
8 Q. Luo, A. Hossen, D. E. Sameen, S. Ahmed, J. Dai, S. Li, W. Qin and Y. Liu, *Crit. Rev. Food Sci. Nutr.*, 2023, **63**, 1102–1118.
9 A. T. Pandian, S. Chaturvedi and S. Chakraborty, *J. Food Meas. Charact.*, 2021, **15**, 1523–1540.
10 S. Forghani, H. Almasi and M. Moradi, *Innovative Food Sci. Emerging Technol.*, 2021, **73**, 102804.
11 S. Wang, X. Liu, M. Yang, Y. Zhang, K. Xiang and R. Tang, *Packag. Technol. Sci.*, 2015, **28**, 839–867.
12 S. Banerjee, C. Kelly, J. P. Kerry and D. B. Papkovsky, *Trends Food Sci. Technol.*, 2016, **50**, 85–102.
13 A. Mills, *Chem. Soc. Rev.*, 2005, **34**, 1003.
14 D. B. Papkovsky and J. P. Kerry, *Sensors*, 2023, **23**, 4519.
15 X. Meng, S. Kim, P. Puligundla and S. Ko, *J. Korean Soc. Appl. Biol. Chem.*, 2014, **57**, 723–733.
16 S. Neethirajan, D. S. Jayas and S. Sadistap, *Food Bioprocess Technol.*, 2009, **2**, 115–121.

17 D. S. Lee, *Trends Food Sci. Technol.*, 2016, **57**, 146–155.
18 P. Puligundla, J. Jung and S. Ko, *Food Control*, 2012, **25**, 328–333.
19 S. Givanoudi, M. Heyndrickx, T. Depuydt, M. Khorshid, J. Robbens and P. Wagner, *Sensors*, 2023, **23**, 613.
20 K. Miller, C. L. Reichert and M. Schmid, *Food Rev. Int.*, 2021, 1–25.
21 D. Gomes Müller, E. Quadro Oreste, M. Grazielle Heinemann, D. Dias and F. Kessler, *Eur. Polym. J.*, 2022, **175**, 111221.
22 R. S. Andre, L. A. Mercante, M. H. M. Facure, R. C. Sanfelice, L. Fugikawa-Santos, T. M. Swager and D. S. Correa, *ACS Sens.*, 2022, **7**, 2104–2131.
23 M. H. S. Santos, *Int. J. Food Microbiol.*, 1996, **29**, 213–231.
24 M. Schirone, L. Esposito, F. D'Onofrio, P. Visciano, M. Martuscelli, D. Mastrocola and A. Paparella, *Foods*, 2022, **11**, 788.
25 K. B. Biji, C. N. Ravishankar, R. Venkateswarlu, C. O. Mohan and T. K. S. Gopal, *J. Food Sci. Technol.*, 2016, **53**, 2210–2218.
26 W. Wójcik, M. Łukasiewicz-Mierzejewska, K. Damaziak and D. Bień, *Animals*, 2022, **12**, 1577.
27 S. M. Khodaei, M. Gholami-Ahangaran, I. Karimi Sani, Z. Esfandiari and H. Eghbaljoo, *Vet. Med. Sci.*, 2023, **9**, 481–493.
28 R. Abedi-Firoozjah, S. A. Salim, S. Hasanvand, E. Assadpour, M. Azizi-Lalabadi, M. A. Prieto and S. M. Jafari, *Compr. Rev. Food Sci. Food Saf.*, 2023, **22**, 1438–1461.
29 F. Boukid, *Coatings*, 2022, **12**, 1949.
30 P. Madhusudan, N. Chellukuri and N. Shivakumar, *Mater. Today Proc.*, 2018, **5**, 21018–21022.
31 D. Schaefer and W. M. Cheung, *Procedia CIRP*, 2018, **72**, 1022–1027.
32 H. Yousefi, H. M. Su, S. M. Imani, K. Alkhaldi, C. D. M. Filipe and T. F. Didar, *ACS Sens.*, 2019, **4**, 808–821.
33 P. Müller and M. Schmid, *Foods*, 2019, **8**, 16.
34 H. Xiao-wei, L. Zhi-hua, Z. Xiao-bo, S. Ji-yong, M. Han-ping, Z. Jie-wen, H. Li-min and M. Holmes, *Food Chem.*, 2016, **197**, 930–936.
35 D. Sriramulu and S. Valiyaveettil, *Dyes Pigm.*, 2016, **134**, 306–314.
36 C. Paoletti, M. He, P. Salvo, B. Melai, N. Calisi, M. Mannini, B. Cortigiani, F. G. Bellagambi, T. M. Swager, F. Di Francesco and A. Pucci, *RSC Adv.*, 2018, **8**, 5578–5585.
37 S. K. Kannan, B. Ambrose, S. Sudalaimani, M. Pandiaraj, K. Giribabu and M. Kathiresan, *Anal. Methods*, 2020, **12**, 3438–3453.
38 C. Calvino, M. Piechowicz, S. J. Rowan, S. Schrettl and C. Weder, *Chem. – Eur. J.*, 2018, **24**, 7369–7373.
39 Y. J. Diaz, Z. A. Page, A. S. Knight, N. J. Treat, J. R. Hemmer, C. J. Hawker and J. Readde Alaniz, *Chem. – Eur. J.*, 2017, **23**, 3562–3566.
40 C. Schaude, C. Meindl, E. Fröhlich, J. Attard and G. J. Mohr, *Talanta*, 2017, **170**, 481–487.
41 M. K. Morsy, K. Zór, N. Kostesha, T. S. Alstrøm, A. Heiskanen, H. El-Tanahi, A. Sharoba, D. Papkovsky, J. Larsen, H. Khalaf, M. H. Jakobsen and J. Emnéus, *Food Control*, 2016, **60**, 346–352.
42 Y. J. Jin and G. Kwak, *Sens. Actuators, B*, 2018, **271**, 183–188.
43 J. Yu and C. Zhang, *J. Mater. Chem. C*, 2020, **8**, 16463–16469.
44 M. Gao, S. Li, Y. Lin, Y. Geng, X. Ling, L. Wang, A. Qin and B. Z. Tang, *ACS Sens.*, 2016, **1**, 179–184.
45 Y. J. Zhao, K. Miao, Z. Zhu and L. J. Fan, *ACS Sens.*, 2017, **2**, 842–847.
46 Y. Meng, C. Yuan, C. Du, K. Jia, C. Liu, K. P. Wang, S. Chen and Z. Q. Hu, *Spectrochim. Acta, Part A*, 2021, **262**, 120152.
47 V. R. Heerthana and R. Preetha, *Rev. Aquacult.*, 2019, **11**, 220–233.
48 N. Kaur, S. Chopra, G. Singh, P. Raj, A. Bhasin, S. K. Sahoo, A. Kuwar and N. Singh, *J. Mater. Chem. B*, 2018, **6**, 4872–4902.
49 Z. Li, S. Hou, H. Zhang, Q. Song, S. Wang and H. Guo, *Adv. Agrochem*, 2023, **2**, 79–87.
50 L. Wang, X. Ran, H. Tang and D. Cao, *Dyes Pigm.*, 2021, **194**, 109634.
51 K. Zhang, H. Li, W. Wang, J. Cao, N. Gan and H. Han, *ACS Sens.*, 2020, **5**, 3721–3738.
52 K. Kivirand and T. Rinken, *Anal. Lett.*, 2011, **44**, 2821–2833.
53 H. Vasconcelos, L. C. C. Coelho, A. Matias, C. Saraiva, P. A. S. Jorge and J. M. M. M. de Almeida, *Biosensors*, 2021, **11**, 82.
54 S. Kashyap, N. Tehri, N. Verma, A. Gahlaut and V. Hooda, *3 Biotech*, 2023, **13**, 2.
55 A. Loutfi, S. Coradeschi, G. K. Mani, P. Shankar and J. B. B. Rayappan, *J. Food Eng.*, 2015, **144**, 103–111.
56 X. Yang, B. Feng, X. He, F. Li, Y. Ding and J. Fei, *Microchim. Acta*, 2013, **180**, 935–956.
57 R. Torre, E. Costa-Rama, H. P. A. Nouws and C. Delerue-Matos, *Biosensors*, 2020, **10**, 139.
58 R. M. Duke, E. B. Veale, F. M. Pfeffer, P. E. Kruger and T. Gunnlaugsson, *Chem. Soc. Rev.*, 2010, **39**, 3936.
59 L. E. Santos-Figueroa, M. E. Moragues, E. Climent, A. Agostini, R. Martínez-Máñez and F. Sancenón, *Chem. Soc. Rev.*, 2013, **42**, 3489.
60 R. Martínez-Máñez and F. Sancenón, *Chem. Rev.*, 2003, **103**, 4419–4476.
61 J. Wu, B. Kwon, W. Liu, E. V. Anslyn, P. Wang and J. S. Kim, *Chem. Rev.*, 2015, **115**, 7893–7943.
62 R. Kato, S. Nishizawa, T. Hayashita and N. Teramae, *Tetrahedron Lett.*, 2001, **42**, 5053–5056.
63 P. Piątek and J. Jurczak, *Chem. Commun.*, 2002, 2450–2451.
64 P. A. Gale, *Acc. Chem. Res.*, 2006, **39**, 465–475.
65 S. P. Mahanta and P. K. Panda, *J. Chem. Sci.*, 2017, **129**, 647–656.
66 J. L. Pablos, S. Fernández-Alonso, F. Catalina and T. Corrales, *Chemosensors*, 2022, **10**, 417.
67 C. R. Harding, J. Cann, A. Laventure, M. Sadeghianlemraski, M. Abd-Ellah, K. R. Rao, B. S. Gelfand, H. Aziz, L. Kaake, C. Risko and G. C. Welch, *Mater. Horiz.*, 2020, **7**, 2959–2969.
68 H. Zhang, X. Wei, M. B. Chan-Park and M. Wang, *ACS Food Sci. Technol.*, 2022, **2**, 703–711.

69 R. Manikandan, N. Shauloff and R. Jelinek, *J. Mater. Chem. C*, 2022, **10**, 16265–16272.
70 T. Soga, Y. Jimbo, K. Suzuki and D. Citterio, *Anal. Chem.*, 2013, **85**, 8973–8978.
71 F. G. Bordwell, *Acc. Chem. Res.*, 1988, **21**, 456–463.
72 D. E. Gómez, L. Fabbrizzi, M. Licchelli and E. Monzani, *Org. Biomol. Chem.*, 2005, **3**, 1495–1500.
73 R. W. G. Hunt and M. R. Pointer, *Measuring Colour*, Wiley, 2011.
74 G. Sharma, W. Wu and E. N. Dalal, *Color Res. Appl.*, 2004, **30**, 21–30.
75 A. R. Robertson, *Color Res. Appl.*, 1977, **2**, 7–11.
76 X. Qi, W. F. Wang, J. Wang, J. L. Yang and Y. P. Shi, *Food Chem.*, 2018, **259**, 245–250.
77 L. Bueno, G. N. Meloni, S. M. Reddy and T. R. L. C. Paixão, *RSC Adv.*, 2015, **5**, 20148–20154.
78 I. Mallov, F. Jeeva and C. B. Caputo, *J. Chem. Technol. Biotechnol.*, 2022, **97**, 830–836.
79 E. K. Feuster and T. E. Glass, *J. Am. Chem. Soc.*, 2003, **125**, 16174–16175.
80 Y. Takagai, Y. Nojiri, T. Takase, W. L. Hinze, M. Butsugan and S. Igarashi, *Analyst*, 2010, **135**, 1417–1425.
81 A. R. Longstreet, M. Jo, R. R. Chandler, K. Hanson, N. Zhan, J. J. Hrudka, H. Mattoussi, M. Shatruk and D. T. McQuade, *J. Am. Chem. Soc.*, 2014, **136**, 15493–15496.
82 L. Dong, C. Deng, C. He, L. Shi, Y. Fu, D. Zhu, H. Cao, Q. He and J. Cheng, *Sens. Actuators, B*, 2013, **180**, 28–34.
83 M. Venkateswarulu, P. Gaur and R. R. Koner, *Sens. Actuators, B*, 2015, **210**, 144–148.
84 P. L. McGrier, K. M. Solntsev, S. Miao, L. M. Tolbert, O. R. Miranda, V. M. Rotello and U. H. F. Bunz, *Chem. – Eur. J.*, 2008, **14**, 4503–4510.
85 T. Han, J. W. Y. Lam, N. Zhao, M. Gao, Z. Yang, E. Zhao, Y. Dong and B. Z. Tang, *Chem. Commun.*, 2013, **49**, 4848.
86 M. Nakamura, T. Sanji and M. Tanaka, *Chem. – Eur. J.*, 2011, **17**, 5344–5349.
87 Y. Che, X. Yang, S. Loser and L. Zang, *Nano Lett.*, 2008, **8**, 2219–2223.
88 J. Zhang, C. Yue, Y. Ke, H. Qu and L. Zeng, *Adv. Agrochem*, 2023, **2**, 127–141.
89 G. Soufi, H. Bagheri, M. Karimi, M. Karimi and S. Jamali, *Anal. Chim. Acta*, 2023, **1238**, 340632.
90 J. Yan, Q. Fu, S. Zhang, X. Shi, Y. Zhang, J. Hou, J. Duan and S. Ai, *New J. Chem.*, 2023, **47**, 7588–7594.
91 P. Ezati, A. Khan, J.-W. Rhim, J. T. Kim and R. Molaei, *Colloids Surf., B*, 2023, **221**, 113013.
92 X. Miao, C. Wu, F. Li and M. Zhang, *Adv. Funct. Mater.*, 2023, 2212980.
93 G. Ding, X. Wang, C. Ling-hu, Y. Fan, L. Zhou, D. Luo, S. Meng, J. Meng, W. Chen, Y. Liu, G. Gao and D. Peng, *Tetrahedron*, 2023, **134**, 133306.
94 A. Gupta, *ChemistrySelect*, 2019, **4**, 12848–12860.
95 M. Gao and B. Z. Tang, *ACS Sens.*, 2017, **2**, 1382–1399.
96 G. Zhang, A. S. Loch, J. C. M. Kistemaker, P. L. Burn and P. E. Shaw, *J. Mater. Chem. C*, 2020, **8**, 13723–13732.
97 Y. Duan, Y. Liu, H. Han, H. Geng, Y. Liao and T. Han, *Spectrochim. Acta, Part A*, 2022, **266**, 120433.
98 B. Razavi, H. Roghani-Mamaqani and M. Salami-Kalajahi, *ACS Appl. Mater. Interfaces*, 2022, **14**, 41433–41446.
99 D. Basavaraja, D. Dey, T. L. Varsha, C. T. Salfeena, M. K. Panda and S. B. Somappa, *ACS Appl. Bio Mater.*, 2020, **3**, 772–778.
100 X.-N. Qi, Y. X. Che, W. J. Qu, Y. M. Zhang, H. Yao, Q. Lin and T.-B. Wei, *Sens. Actuators, B*, 2021, **333**, 129430.
101 S. Bettini, Z. Syrgiannis, R. Pagano, L. Dordevic, L. Salvatore, M. Prato, G. Giancane and L. Valli, *ACS Appl. Mater. Interfaces*, 2019, **11**, 17079–17089.
102 H. Peng, L. Ding, T. Liu, X. Chen, L. Li, S. Yin and Y. Fang, *Chem. – Asian J.*, 2012, **7**, 1576–1582.
103 B. Zhang, H. Soleimaninejad, D. J. Jones, J. M. White, K. P. Ghiggino, T. A. Smith and W. W. H. Wong, *Chem. Mater.*, 2017, **29**, 8395–8403.
104 J. Royakkers, A. Minotto, D. G. Congrave, W. Zeng, A. Hassan, A. Leventis, F. Cacialli and H. Bronstein, *Chem. Mater.*, 2020, **32**, 10140–10145.
105 F. Zhang, Y. Ma, Y. Chi, H. Yu, Y. Li, T. Jiang, X. Wei and J. Shi, *Sci. Rep.*, 2018, **8**, 8208.
106 F. Würthner, C. R. Saha-Möller, B. Fimmel, S. Ogi, P. Leowanawat and D. Schmidt, *Chem. Rev.*, 2016, **116**, 962–1052.
107 R. Hu, S. Li, Y. Zeng, J. Chen, S. Wang, Y. Li and G. Yang, *Phys. Chem. Chem. Phys.*, 2011, **13**, 2044–2051.
108 M. Gao, Q. Hu, G. Feng, B. Z. Tang and B. Liu, *J. Mater. Chem. B*, 2014, **2**, 3438–3442.
109 R. Roy, N. R. Sajeev, V. Sharma and A. L. Koner, *ACS Appl. Mater. Interfaces*, 2019, **11**, 47207–47217.
110 S. K. Behera, S. Y. Park and J. Gierschner, *Angew. Chem., Int. Ed.*, 2021, **60**, 22624–22638.
111 S. Mukherjee and P. Thilagar, *Chem. – Eur. J.*, 2014, **20**, 9052–9062.
112 A. E. D. A. Bekhit, B. W. B. Holman, S. G. Giteru and D. L. Hopkins, *Trends Food Sci. Technol.*, 2021, **109**, 280–302.
113 S. P. Bernier, S. Létoffé, M. Delepierre and J. M. Ghigo, *Mol. Microbiol.*, 2011, **81**, 705–716.
114 M. R. Pinto, C. Tan, M. B. Ramey, J. R. Reynolds, T. S. Bergstedt, D. G. Whitten and K. S. Schanze, *Res. Chem. Intermed.*, 2007, **33**, 79–90.
115 K. Lee, L. K. Povlich and J. Kim, *Analyst*, 2010, **135**, 2179.
116 J. Sinha and A. Kumar, *Synth. Met.*, 2010, **160**, 2265–2272.
117 C. S. Tsai, S. H. Yang, B. C. Liu and H. C. Su, *Org. Electron.*, 2013, **14**, 488–499.
118 A. Garcia, Y. Jin, J. Z. Brzezinski and T. Q. Nguyen, *J. Phys. Chem. C*, 2010, **114**, 22309–22315.
119 J. H. Ortony, R. Q. Yang, J. Z. Brzezinski, L. Edman, T. Q. Nguyen and G. C. Bazan, *Adv. Mater.*, 2008, **20**, 298–302.
120 M. Kang, O. K. Nag, R. R. Nayak, S. Hwang, H. Suh and H. Y. Woo, *Macromolecules*, 2009, **42**, 2708–2714.
121 S. Rochat and T. M. Swager, *Angew. Chem., Int. Ed.*, 2014, **53**, 9792–9796.
122 P. C. Jurs, G. A. Bakken and H. E. McClelland, *Chem. Rev.*, 2000, **100**, 2649–2678.
123 S. Rochat, J. Gao, X. Qian, F. Zaubitzer and K. Severin, *Chem. – Eur. J.*, 2010, **16**, 104–113.

124 S. W. Thomas III, J. P. Amara, R. E. Bjork and T. M. Swager, *Chem. Commun.*, 2005, 4572.
125 R. Jia, W. Tian, H. Bai, J. Zhang, S. Wang and J. Zhang, *Nat. Commun.*, 2019, **10**, 795.
126 C. O. R. Okpala, W. S. Choo and G. A. Dykes, *LWT Food Sci. Technol.*, 2014, **55**, 110–116.
127 G. Das, B. Garai, T. Prakasam, F. Benyettou, S. Varghese, S. K. Sharma, F. Gándara, R. Pasricha, M. Baias, R. Jagannathan, N. Saleh, M. Elhabiri, M. A. Olson and A. Trabolsi, *Nat. Commun.*, 2022, **13**, 3904.
128 S. Nandi, S. Mandal, J. S. Matalobos, A. Sahana and D. Das, *J. Mol. Recognit.*, 2016, **29**, 5–9.
129 J. Zhang, D. Yue, T. Xia, Y. Cui, Y. Yang and G. Qian, *Microporous Mesoporous Mater.*, 2017, **253**, 146–150.
130 C. Bao, S. Shao, H. Zhou and Y. Han, *New J. Chem.*, 2021, **45**, 10735–10740.
131 Y. Liu, Y. Xiao, M. Shang, Y. Zhuang and L. Wang, *Chem. Eng. J.*, 2022, **428**, 132647.
132 A. P. Côté, A. I. Benin, N. W. Ockwig, M. O'Keeffe, A. J. Matzger and O. M. Yaghi, *Science*, 2005, **310**, 1166–1170.
133 Y. Sun, B. Zhang, C. Zhang, H. Lu, Y. Yang, B. Han, F. Dong, J. Lv, S. Zhang, Z. Li, Z. Lei and H. Ma, *ACS Appl. Mater. Interfaces*, 2023, **15**, 4569–4579.
134 R. A. Potyrailo, N. Nagraj, Z. Tang, F. J. Mondello, C. Surman and W. Morris, *J. Agric. Food Chem.*, 2012, **60**, 8535–8543.
135 Z. Meng and Z. Li, *Meas. Sci. Rev.*, 2016, **16**, 305–315.
136 R. J. Rath, S. Farajikhah, F. Oveissi, F. Dehghani and S. Naficy, *Adv. Eng. Mater.*, 2023, **25**, 2200830.
137 J. Lin, M. Kilani and G. Mao, *Adv. Mater. Technol.*, 2023, **8**, 2202038.
138 A. K. Singh, N. K. Chowdhury, S. C. Roy and B. Bhowmik, *J. Electron. Mater.*, 2022, **51**, 1974–2003.
139 Y. Wang, J. Zhang, S. Zhang and J. Huang, *Polym. Int.*, 2021, **70**, 414–425.
140 Z. Ma, P. Chen, W. Cheng, K. Yan, L. Pan, Y. Shi and G. Yu, *Nano Lett.*, 2018, **18**, 4570–4575.
141 L. K. Fiddes, J. Chang and N. Yan, *Sens. Actuators, B*, 2014, **202**, 1298–1304.
142 M. A. Rahman, P. Kumar, D. S. Park and Y. B. Shim, *Sensors*, 2008, **8**, 118–141.
143 A. Nasri, M. Pétrissans, V. Fierro and A. Celzard, *Mater. Sci. Semicond. Process.*, 2021, **128**, 105744.
144 S. Park, C. Park and H. Yoon, *Polymers*, 2017, **9**, 155.
145 X. Zhou, S. Lee, Z. Xu and J. Yoon, *Chem. Rev.*, 2015, **115**, 7944–8000.
146 R. Abbel, Y. Galagan and P. Groen, *Adv. Eng. Mater.*, 2018, **20**, 1701190.
147 Z. Yin, Y. Huang, H. Yang, J. Chen, Y. Duan and W. Chen, *Sci. China: Technol. Sci.*, 2022, **65**, 1940–1956.
148 J. Bian, L. Zhou, X. Wan, C. Zhu, B. Yang and Y. Huang, *Adv. Electron. Mater.*, 2019, **5**, 1800900.
149 P. Mougkogiannis, M. Turner and K. Persaud, *Sensors*, 2020, **21**, 13.
150 Y. Yang, G. Zhang, H. Luo, J. Yao, Z. Liu and D. Zhang, *ACS Appl. Mater. Interfaces*, 2016, **8**, 3635–3643.
151 L. K. Fiddes and N. Yan, *Sens. Actuators, B*, 2013, **186**, 817–823.
152 J. M. Schnorr and T. M. Swager, *Chem. Mater.*, 2011, **23**, 646–657.
153 P. M. Ajayan, *Chem. Rev.*, 1999, **99**, 1787–1800.
154 R. H. Baughman, A. A. Zakhidov and W. A. de Heer, *Science*, 2002, **297**, 787–792.
155 W. A. de Heer, *MRS Bull.*, 2004, **29**, 281–285.
156 T. Zhang, S. Mubeen, N. V. Myung and M. A. Deshusses, *Nanotechnology*, 2008, **19**, 332001.
157 J. M. Azzarelli, K. A. Mirica, J. B. Ravnsbæk and T. M. Swager, *Proc. Natl. Acad. Sci. U. S. A.*, 2014, **111**, 18162–18166.
158 L. C. Wang, K. T. Tang, I. J. Teng, C. T. Kuo, C. L. Ho, H. W. Kuo, T. H. Su, S. R. Yang, G.-N. Shi and C. P. Chang, *Sensors*, 2011, **11**, 7763–7772.
159 N. Calisi, P. Salvo, B. Melai, C. Paoletti, A. Pucci and F. Di Francesco, *Mater. Chem. Phys.*, 2017, **186**, 456–461.
160 P. Salvo, N. Calisi, B. Melai, V. Dini, C. Paoletti, T. Lomonaco, A. Pucci, F. Di Francesco, A. Piaggesi and M. Romanelli, *Int. J. Nanomed.*, 2017, **12**, 949–954.
161 S. F. Liu, A. R. Petty, G. T. Sazama and T. M. Swager, *Angew. Chem., Int. Ed.*, 2015, **54**, 6554–6557.
162 Y. G. Kim, B. M. Oh, H. Kim, E. H. Lee, D. H. Lee, J. H. Kim and B. Koo, *Sens. Actuators, B*, 2022, **367**, 132076.
163 L. Y. Chang, M. Y. Chuang, H. W. Zan, H. F. Meng, C. J. Lu, P. H. Yeh and J. N. Chen, *ACS Sens.*, 2017, **2**, 531–539.
164 S. Agbolaghi and S. Zenoozi, *Org. Electron.*, 2017, **51**, 362–403.
165 S. Zhang, Y. Zhao, X. Du, Y. Chu, S. Zhang and J. Huang, *Small*, 2019, **15**, 1805196.
166 A. Lv, Y. Pan and L. Chi, *Sensors*, 2017, **17**, 213.
167 Z. Wang, Z. Liu, L. Chen, Y. Yang, J. Ma, X. Zhang, Y. Guo, G. Zhang and D. Zhang, *Adv. Electron. Mater.*, 2018, **4**, 1800025.
168 D. J. Tate, E. Danesh, V. Tischler, S. Faraji, L. A. Majewski, M. L. Turner and K. C. Persaud, *2017 ISOCS/IEEE International Symposium on Olfaction and Electronic Nose (ISOEN)*, 2017, 1–3.
169 A. Rahmanudin, D. J. Tate, R. Marcial-Hernandez, N. Bull, S. K. Garlapati, A. Zamhuri, R. U. Khan, S. Faraji, S. R. Gollu Krishna, C. Persaud and M. L. Turner, *Adv. Electron. Mater.*, 2020, **6**, 1901127.
170 S. Choi, F. A. Larrain, C. Y. Wang, C. Fuentes-Hernandez, W. F. Chou and B. Kippelen, *J. Mater. Chem. C*, 2016, **4**, 8297–8303.
171 V. R. Rajeev, A. K. Paulose and K. N. N. Unni, *Vacuum*, 2018, **158**, 271–277.
172 T. Minamiki, Y. Hashima, Y. Sasaki and T. Minami, *Chem. Commun.*, 2018, **54**, 6907–6910.
173 A. Laiho, L. Herlogsson, R. Forchheimer, X. Crispin and M. Berggren, *Proc. Natl. Acad. Sci. U. S. A.*, 2011, **108**, 15069–15073.